Accepted Manuscript

Substituted tetrahydroisoquinolines: synthesis, characterization, antitumor activity and other biological properties

A. Sergi Capilla, Richard Soucek, Laura Grau, Manel Romero, Jaime Rubio-Martínez, Daniel H. Caignard, Maria Dolors Pujol

PII: S0223-5234(17)31129-7

DOI: 10.1016/j.ejmech.2017.12.098

Reference: EJMECH 10076

To appear in: *European Journal of Medicinal Chemistry*

Received Date: 1 September 2017

Revised Date: 29 December 2017

Accepted Date: 30 December 2017

Please cite this article as: A.S. Capilla, R. Soucek, L. Grau, M. Romero, J. Rubio-Martínez, D.H. Caignard, M.D. Pujol, Substituted tetrahydroisoquinolines: synthesis, characterization, antitumor activity and other biological properties, *European Journal of Medicinal Chemistry* (2018), doi: 10.1016/j.ejmech.2017.12.098.

Substituted tetrahydroisoquinolines: synthesis, characterization, antitumor activity and other biological properties

A. Sergi Capilla, Richard Soucek, Laura Grau, Manel Romero, Jaime Rubio-Martínez, Daniel H. Caignard, and Maria Dolors Pujol

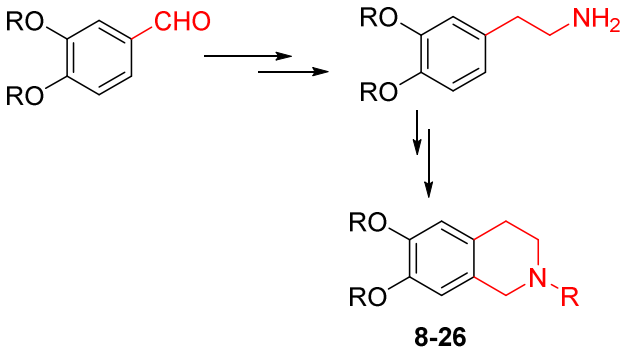

8-26

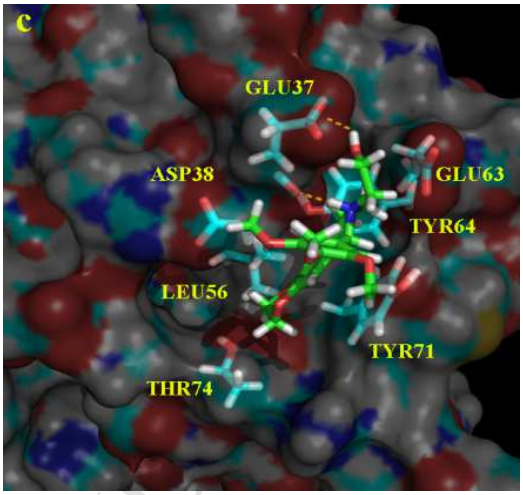

- 18 Dioxigenated tetradydroisoquinoline compounds were synthesized from the corresponding aldehyde.
- Compounds **12**, **13**, **14**, **15**, **16**, **18**, **20** and **21** exhibited significant cytotoxic activity.
- Isoquinoline **14** presents the best KRas activity profile on RKO KRasSL.
- Molecular modeling studies showed that the tetrahydroisoquinoline **12** binds directly to the p1 pocket of the KRas protein.

Substituted tetrahydroisoquinolines: synthesis, characterization, antitumor activity and other biological properties

A. Sergi Capilla,[#] Richard Soucek,[#] Laura Grau,[#] Manel Romero,[#] Jaime Rubio-Martínez,[§] Daniel H. Caignard,[¥] and Maria Dolors Pujol[#]*

[#] Laboratori de Química Farmacèutica (Unitat associada al CSIC). Facultat de Farmàcia, Universitat de Barcelona, Spain.

[§] Department of Physical Chemistry, Faculty of Chemistry, University of Barcelona and the Institut de Recerca en Química Teòrica i Computacional (IQTCUB), Barcelona, Spain.

[¥] Les laboratoires Servier. 1 rue Carle Hébert-92415 Courbevoie cedex. 92200 Neuilly-sur Seine (France)

Keywords: Isoquinolines, Dioxigenated compounds, Antitumor, KRas, Molecular Dynamics, Allosteric Sites, Drug Design.

Abstract. This work deals with the molecular design, synthesis and biological activity of a series of tetrahydro[1,4]dioxanisoquinolines and dimethoxyisoquinoline analogues. This study describes the synthesis strategy of these potential antitumor compounds, their multi-step synthesis and their optimization. A series of tetrahydroisoquinolines was synthesized and their cytotoxicity evaluated.

Some of these tetrahydroisoquinolines showed promising KRas inhibition, antiangiogenesis activity and antiosteoporosis properties. Molecular modeling studies showed that compound **12** bind in the p1 pocket of the KRas protein making interactions with the hydrophobic residues Leu56, Tyr64, Tyr71 and Thr74 and hydrogen bonds with residues Glu37 and Asp38.

1. Introduction

Substituted *N*-heterocycles systems like indole, azaindole, quinolone, isoquinoline and piperidine analogues are structural subunits present in numerous natural and synthetic compounds exhibiting a wide range of biological activities [1]. Among them the tetrahydroisoquinoline core in particular is widely studied as a scaffold for the preparation of potential therapeutically active compounds [2]. This heterocycle can be found in several drugs, such as *noscapine*, a natural benzyl tetrahydroisoquinoline alkaloid considered antitussive and also exhbits antitumor and antiisquemic properties [3], *solifenacin*, an antimuscarinic agent that is used for the treatment of overactive bladder [4] and EDL-155 showed an anti-glioma profile (Figure 1) [5].

The tetrahydroisoquinoline heterocycle is a privileged scaffold in the antitumor agents [6] that may be introduced in the structures with potential antitumor activity by KRas inhibition [6]. It is known that KRas inhibition plays an important role in the treatment of diverse cancer diseases such as leukemia, lung adenocarcinoma, pancreas and colorectal adenocarcinoma. As a consequence, the preparation of small molecules that bind to the KRas proteins has stimulated considerable interest. A key feature of this research is the preparation of small structures possessing an isoquinoline nucleus condensed with the 1,4-dioxan ring which must contribute with two sites of modest polarity.

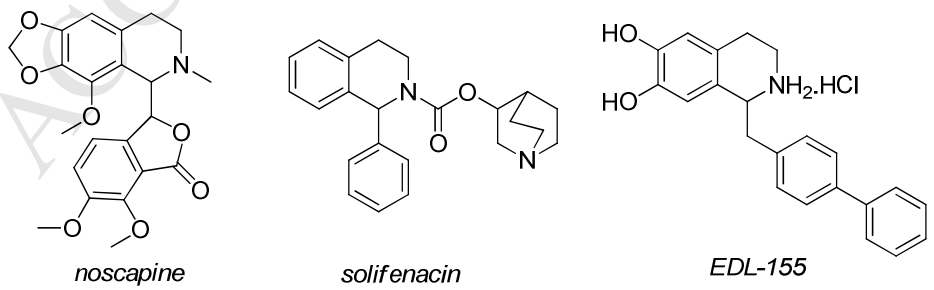

Figure 1. Bioactive isoquinolines

2. Results and discussion

2.1. Chemistry

Classical methods for preparing tetrahydroisoquinolines consist of intramolecular electrophilic aromatic cyclization of arylethylamides under Bischler Napieralski conditions followed by reduction [7]. A while ago, we developed a direct access to tetrahydroisoquinolines by cyclization of an imine intermediate under acid catalysis, affording acylated tetrahydroisoquinolines in good to high yields [8].

Target tetrahydroisoquinolines were synthesized as racemic mixtures according to the sequence of reactions indicated in Schemes 1-4.

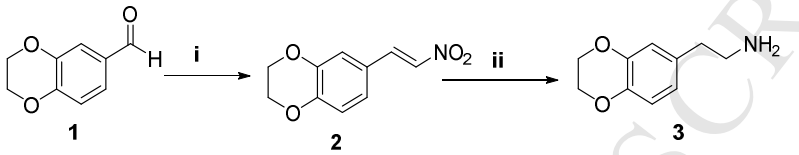

Reagents and conditions: i) CH_3NO_2 (10 mL), CH_3COONH_4 (3.5 eq), 100 °C, 2 h, 99%. ii) Pd/C (10% w/w), H_2 (7 atm), MeOH/EtOAc 1:3, 16 h, 53% or $LiAlH_4$ (4 eq), THF, rt, 16 h, 61%.

Scheme 1. Synthesis of compound **3**

The aldehyde **1** reacted with nitromethane and ammonium acetate according to the literature procedure to afford **2** in excellent yield [9]. Reduction of the nitroethene **2** under hydrogen stream in the presence of Pd/C led mostly to the vinyl amine and only traces of the amine **3**. Hydrogenation of **2** (6-8 atm) with Pd/C slightly improved the reduction to **3** in 53% yield. Finally, the reduction of **2** with $LiAlH_4$ under classical conditions afforded the amine **3** in acceptable yield (61%) (Scheme 1). Using the last reduction procedure the overall yield of these 2-steps reaction was 61%.

The tetrahydroisoquinolines **8**-**9** were synthesized following our previously reported procedure [8]. Amination of 3,4,5-trimethoxybenzaldehyde (**4**) with the arylethylamine **3** using PTSA (*p*-toluensulfonic acid) or CSA (canforsulfonic acid) in toluene did not yield the corresponding isoquinoline due to solubility problems. However, treatment of the aldehyde **4** with the amine **3** in EtOH at p*H* 6 in presence of molecular sieves 4 Å, followed by an intramolecular cyclization reaction of the resulting imine with TFA (trifluoroacetic acid) and TFAA (trifluoroacetic anhydride) gave the intermediate **6** which after hydrolysis with NaOH 2N gave the dioxine-isoquinoline **8** in 97% yield.

An alternative was tried to improve the yield of **8**. Amination of the 3,4,5-trimethoxybenzaldehyde **4** with the arylethylamine **3** in a Dean Stark apparatus, followed by addition of H_3PO_4 (85% in aqueous solution) afforded the isoquinoline **8** in 32% yield (Scheme 3). From the phenethylamine **3** and the 4-pyridinyl carbaldehyde **5** following the same procedure the isoquinoline **9** was obtained in acceptable yield [8]. The oxidation of **8** with Pd in quinoline gave the isoquinoline **10** in moderate yield.

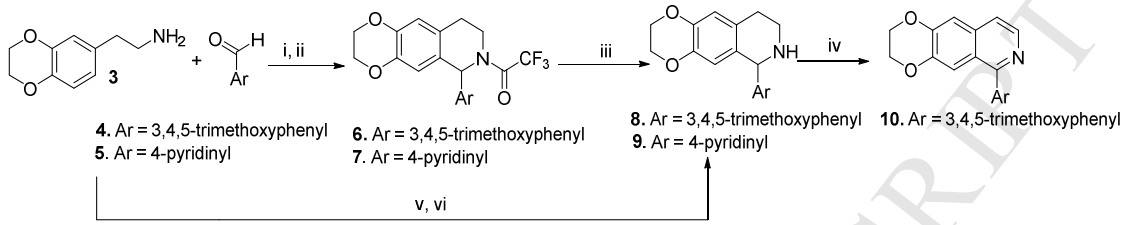

Reagents and conditions: i) toluene, PTSA, Dean Stark, 16 h, reflux. ii) TFA, TFAA, rt, 16 h, 33%. iii) NaOH 2N/MeOH 7:3, reflux, 16 h, 97% from **6**. iii) NaOH 2N, MeOH, reflux, 16 h, 98% from **7**. iv) Pd, quinoline, 200 ºC.

Alternative method: v) 3,4,5-trimethoxybenzaldehyde (1.1 eq), benzene, Dean-Stark, 110 °C, 3 h. vi) H_3PO_4 (2 mL of a 85% aqueous solution), Dean-Stark, 110 °C, 4 h, 32% yield.

Scheme 2. Synthesis of the dioxinisoquinolines **8**-**10**

The isoquinoline **8** was involved in an alkylation process using classical conditions. In a general procedure, **8** and **9** were treated with the corresponding alkyl halide, Et_3N or K_2CO_3, KI and DMF to obtain the desired compounds in low to satisfactory yields.

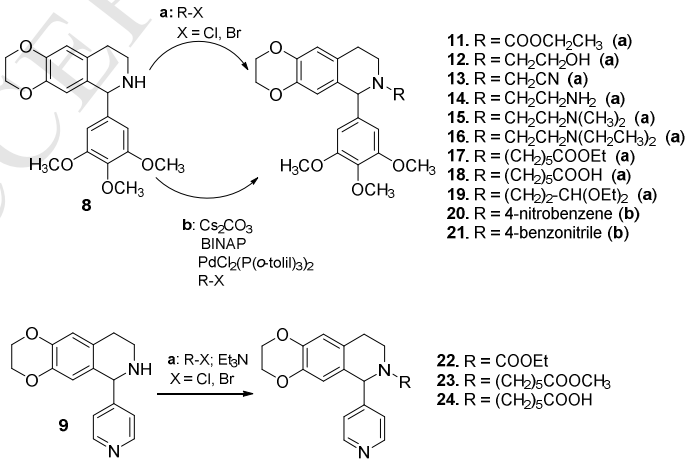

Reagents and conditions: a) R-X (25 eq over 7 days), Et_3N (8 eq), KI (0.1 eq), rt, DMF. b) $PdCl_2((o\text{-tolyl})_3P)_2$, (±)-BINAP and Cs_2O_3

Scheme 3. Synthesis of the dioxinisoquinolines **11-24**

The results of a number of alkylation attempts of **8** carried out revealed better yields when performed at room temperature despite of an increased reaction time. Indeed, alkylation of **8** at 80 °C was faster but favored the oxidation of the tetrahydroisoquinoline **8** to the isoquinoline **10.**

The acylation of **8** under classical conditions gave the chloroformate **11** in acceptable yield (79%). The tetrahydroisoquinoline **8** was alkylated with 2-chloroethanol under classical conditions in the presence of Et_3N and KI providing the alcohol **12** in 32% yield after purification.

Alkylation of **8** using chloroacetonitrile gives **13** in a satisfactory yield (84%). The nitrile group of **13** was reduced with $LiAlH_4$ to yield **14** in acceptable yield.

The tetrahydroisoquinoline **8** was involved in an *N*-alkylation reaction under the same reaction conditions as indicated above with 2-dimethylaminoethyl chloride, Et_3N and KI to afford **15** in 54% yield. The hyrolysis of **17** with aqueous NaOH solution provided the caraboxylic acid **18** in acceptable yield. Using the same conditions **15** and **16** were obtained from **8** in 25 and 46% respectively. The acetal **19** was synthesized by *N*-alkylation of **8** with the corresponding alkyl halide in low yield.

The preparation of the tetrahydroisoquinolines **20** and **21** was accomplished by *N*-arylation of the tetrahydroisoquinoline **8** following a general procedure described in the literature [10]. The tetrahydroisoquinoline **8** reacted with 1-bromo-4-nitrobenzene in the presence of $PdCl_2((o\text{-tolyl})_3P)_2$, (±)-BINAP and Cs_2O_3 in toluene yielding **20** in 33% yield. In the same way, the *N*-arylation of **8** with 4-bromobenzonitrile afforded **21** in 26% yield (Scheme 3). The low yields should be attributed to the hindrance provided by the trimethoxyphenyl substituent at the C-1 position as well as the high temperature required for this *N*-arylation that favored the formation of the aromatized isoquinoline **10**.

The pyridine derivatives **22-24** were obtained using similar conditions to those employed for the preparation of **11**, **17** and **18** respectively.

In order to determine if the substitution of the 1-4-dioxane nucleus by a dimethoxy group results in an increase or decrease in biological activity, two dimethoxy-isoquinoline analogues were synthesized from the commercially available 2-(3,4-dimethoxyphenyl)ethylamine **29** following the

same experimental protocol used for the preparation of the isoquinoline **8**. 3,4,5-Trimethoxybenzaldehyde (**4**) and 2-(3,4-dimethoxyphenyl)ethylamine (**29**) were coupled under amination reaction conditions, followed by intramolecular cyclization of the corresponding imine with TFA and TFAA to afford the amide **26** in moderate yield. The tetrahydroisoquinoline **27** was prepared from hydrolysis of **28** with NaOH 2N in satisfactory yield (Scheme 4).

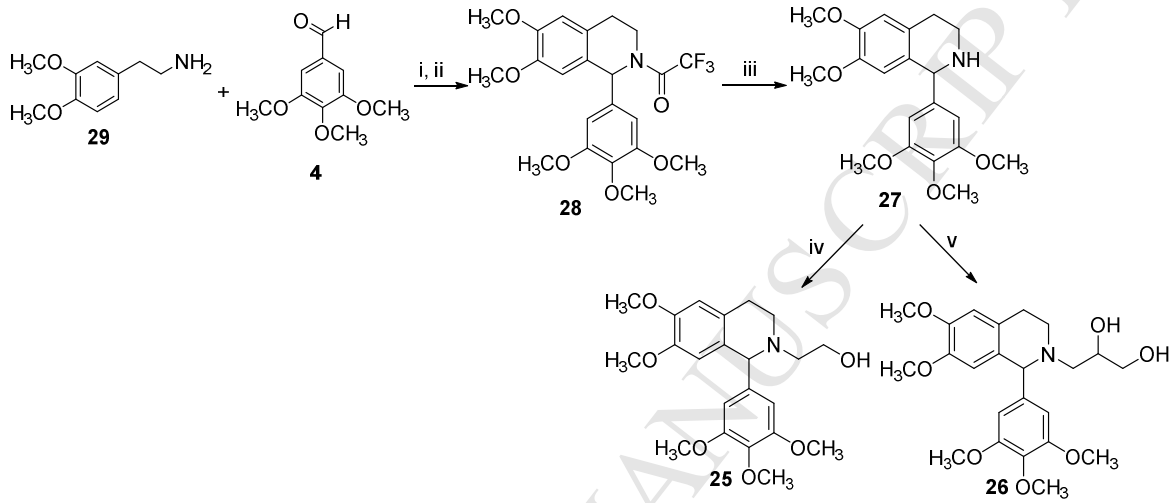

Reagents and conditions: i) toluene, PTSA, Dean Stark, 16 h, reflux. ii) TFA, TFAA, rt, 16 h, 33%. iii) NaOH 2N/MeOH 7:3, reflux, 16 h, 97%. iv) 2-chloroethanol (25 eq over 7 days), Et_3N (8 eq), KI (0.1 eq), rt, DMF, 10 days, 16%. v) 1) *(±)*-epichlorohydrin (9 eq over 2 days), Et_3N (8 eq), KI (0.1 eq), rt, DMF, 2 days, 45%. 2) NaOH 2N/1,4-dioxane 5:2, rt, 2 days, 48%.

Scheme 4. Synthesis of isoquinolines **25** and **26**

The dimethoxyisoquinoline **27** was alkylated giving two new compounds. First, treatment of **27** with 2-chloroethanol under classical conditions led to the alcohol **25** in low yield (Scheme 4). The reaction was performed at room temperature because of the same stability problems than the amine **8**.

Similarly, the alkylation of **27** with (±)-epichlorohydrin in the presence of Et_3N and KI led to the intermediate epoxide which was hydrolyzed with NaOH 2N to afford the diol **26** in moderate yield (Scheme 4).

2.2. Biological evaluation

2.2.1. *In vitro* cytotoxic activity on L1210 murine leukemia cell line

In vitro assay was used to screen all the newly synthesized isoquinolines for their effects on tumor cell lines. In this study, we focused on the isoquinoline substituents to evaluate their effect over the biological activities.

Isoquinolines **8** and **10-26** synthesized during this study were tested on L1210 murine leukemia cell line and the compounds **12-16**, **18**, and **20-21** exhibited biologically significant anticancer activity. The cytotoxicity showed by compound **14** was of great interest and also its action over the phase G1 of the cell cycle was remarkable, whereas compounds **8**, **10**, **25** and **26** were much less active and isoquinolines **11**, **17**, **19** and **22-24** were inactive (Table 1). The results show that compounds **25** and **26** showed poor or no inhibition of cancer cell lines growth on the three studied lines.

The structure-activity-relationships between **12** and **25** show that the dimethoxide groups result in a decrease of biological activity compared to the 1,4-benzodioxin moiety. The structure-activity-relationships between **25** and **26** reveals that a diol side chain results in an increase of antitumor activity compared to a terminal alcohol side chain. The presence of amino ethyl group (Table 1, compounds **14** and **15**) as isoquinoline substituent gives selectivity by the phase G1, whereas a hydroxyethyl substituent favors the action over the 8N subphase (Table 1, compound **12**). An aryl as *N*-substituent maintains a good cytotoxic activity (Table 1, compounds **20** and **21**). Curiously the nitrobenzene group (compound **20**) facilitates the action over de phase G1 and the benzonitrile (compound **21**) on the 8N subphase. With respect to the substituent at the C-1 of the tetrahydroisoquinoline, the 3,4,5-trimethoxyphenyl group contributes to a better therapeutic profile than 4-pyridinyl.

Table 1. *In vitro* cytotoxity activity of compounds **8** and **10-26**

Compound	**IC_{50} (μM, L1210)**	**Cycle (L1210)**
8	21.1±3.40	G_1 (+100 μM)
10	25.1±3.20	G_2M+++100 μM
11	>10	Not tested
12	2.6±0.87	70% 8N 5 μM

13	4.2±0.78	G_1 (+100 µM)
14	2.0±0.72	G_1 (+25 µM)
15	3.7±0.66	G_1 (++25 µM)
16	4.1±0.89	Not specific
17	>10	Not tested
18	9.4±1.20	Not specific
19	>10	Not tested
20	4.6±075	G_1 (+25 µM)
21	3.6±0.69	70% 8N 10 µM
22	>10	Not tested
23	>10	Not tested
24	>10	Not tested
25	23.4±2.56	Not specific
26	15.3±2.43	Not specific
Acronycine	21,0±2.01	G2M (++50 µM)

Results are expressed as the mean (n = 3) of L1210 inhibition and expressed by IC_{50}

2.2.2. KRas inhbition

The isoquinolines **12**, **13**, **14**, **20** and **21** were selected for testing at the Eli Lilly Laboratories [11] (Indianapolis, USA) to estimate their antitumor activities and to study their mode of action. The KRas activity of the five tested compounds were carried out on four different colon cancer cell lines (HCT KRasSL, RKO KRasSL, Colo 320 KRasSL and SNU-C1 KRasSL) in three different concentrations (0.2 µM, 2 µM and 20 µM) (Table 2).

Table 2. KRas inhibition of the tetrahydroisoquinoline analogues

Products / Assays	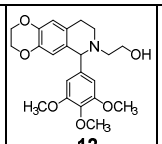 **12**	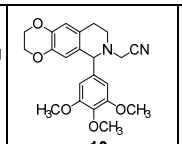 **13**	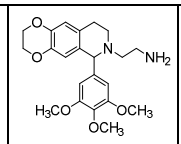 **14**	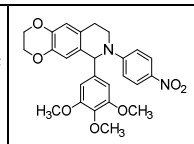 **20**	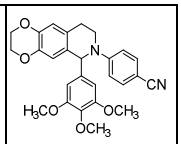 **21**

HCT KRasSL	% In. 0.2 µM	18	12.1	0	0	35.9
	% In. 2 µM	12.1	17.0	16.2	19.3	16.0
	% In. 20 µM	46.5	49.1	56.9	55.9	45.2
RKO KRasSL*	% In.0.2 µM	0	0	0	17.9	95.8
	% In. 2 µM	6.3	16.3	10.1	32.9	7.7
	% In. 20 µM	76.7	79.2	92.7	70.5	66.5
Colon 320 KRasS*	% In. 0.2 µM	12.2	0	0	0	0
	% In. 2 µM	0	8.2	20.1	4	22.5
	% In. 20 µM	78.2	74.7	85.3	92.5	89.9
SNU-C1 KRasSL*	% In. 0.2 µM	12.3	10.0	12.2	17.7	6.6
	% In. 2 µM	11.5	6.0	2.4	35.0	32.5
	% Inhib 20 µM	19.7	59.8	57.1	42.7	43.5

*SNU-C1, Colon 320, RKO and HCT are colon cancer cell lines.

The results show that all of the studied compounds have a higher overall KRas inhibition. Surprisingly, the alcohol **12** displayed a lower KRas inhibition than the other isoquinoline analogues (see Table 2). The amine isoquinoline **14** presents the best KRas activity profile on RKO KRasSL of the tested tetrahydroisoquinoline analogues, which reveals that a terminal ionic interaction leads to an increase of KRas inhibition. The *N*-arylisoquinoline **20** and **21** have the highest KRas inhibition on Colon 320 KRas SL cell line, which suggests that a low electron density aromatic side chain structure results in a higher KRas activity for this type of cancer cells. The isoquinoline **21** shows a surprisingly high KRas activity at 0.2 µM concentration (RKO KRasSL 95.8% inhib., HCT KRasSL 35.9% inhib.) which suggests that its activity is not dose-dependent for these types of cancer cell lines.

2.2.3. Angiogenesis and antiosteoporosis activities

The antiangiogenesis evaluation was carried out for **12**, **13**, **14**, **20** and **21**. The results show that the isoquinolines **13** and **14** possess an interesting antiangiogenic activity while **20** and **21** demonstrated moderate activity and **12** was inactive (Table 3). The nitrile isoquinoline **13** was the most potent

antiangiogenic in this study and shows the highest antiangiogenesis (IC_{50} = 2.9 μM) and antiosteoporosis activity, which suggests that a dipolar lipophilic terminal group such as a nitrile group results in an increase of antiangiogenesis and antiosteoporosis activity (Table 3).

These results suggest that a functionalized group on the side chain bound to the isoquinoline nitrogen atom in general, improves the antitumor properties significantly.

Table 3. Antiangiogenesis and antiosteoporosis activity of the tetrahydroisoquinoline analogues

Assays \ Products			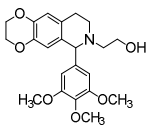 **12**	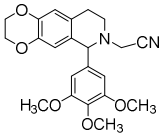 **13**	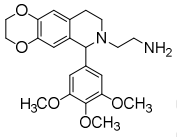 **14**	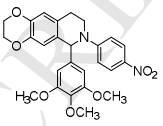 **20**	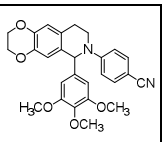 **21**
Antiangiogenesis*	Angio Tube Area	% In. 2 μM	0	15	8.5	6	16.6
		% In. 10 μM	6.7	76.9	58.6	37.5	55.3
		IC_{50}	N.A	2.9 μM	6.5 μM	>10 μM	>10 μM
	Angio Nuc Area	IC_{50}	N.A	>10 μM	>10 μM	>10 μM	>10 μM
	Osteo bCat	%Stim 2 μM	0	4.6	0	0.3	27.2
		%Stim 10 μM	2,9	51,8	25,4	4,3	14,2

*Angiogenesis nuclear area, β-catenin osteoporosis and angiogenesis tube area (tracheal tube area)

3. Molecular Modeling Studies

Because the potency of the compounds described in Tables 2 is different depending on the biological assay and also for having a minimal antiangiogenic effect (Table 3) compound **12** was selected as representative member of the diverse tetrahydroisoquinoline analogues described above for the determination of its most probable binding site to KRas. Bearing this in mind and aimed at exploring the conformational space of the KRas-Lig system [12] thoroughly, ten KRas-Lig_8 different complexes were prepared and subjected to a 100 ns of MD trajectory, as explained in the Methods section. Visual inspection of the MD trajectories shows different possible situations. In some of the calculations none of the eight ligands remains bound to the KRas protein in the last ten nanoseconds; in others, only one ligand is bounded to the KRas protein during the last ten nanoseconds, although

they are found in different pockets; and finally, in some of the calculations more than one ligand remained bound to the KRas protein during the last ten nanoseconds [13]. In the latter case, ligands were bound, in general, in different pockets but found close together due to van der Waals attractive inter-ligands interactions. Once the multiple copies MD calculations were analyzed and aimed at achieving a better understanding of the binding process, avoiding any bias due to the presence of multiple-ligands in the calculations, eighteen complexes with only one ligand, extracted from these calculations (see Molecular Modeling Methods) were used to analyze the behavior of the complex along the molecular dynamics with different starting points having the ligand bound to different sites.

For a clearer discussion about the interactions of the ligand with the KRas protein, Figure 2 shows its most relevant structural motifs together with the different allosteric sites explored in this study. The stating position and the behavior of the ligand along the MD in each of the eighteen studied complexes are described in Table S1 of Supporting Information. Thus, six MD starts at the p1 pocket (MD 1 to 6). However, two of them after different production times leave the protein (MD 3 and 4). The MD 5 and 6 leave the protein but finally return to the protein at different sites. Molecular dynamics 1 and 2 remain at the p1 pocket being the first the most stable of all. Three MD start at the p2 pocket but two of them leave the protein. Four MD start at p4 and they all go. However, two of them return to the hypervariable zone. Also four MD start between helices α-3 and α-4. None of them remain at this position. Finally, one MD start between β2 and β3 strands but go out and return to another place.

In order to determine simulations convergence as well as the stability of the different complexes, the total binding free energy calculated by the MMGBSA approach was plotted as a function of the trajectory length. The plot for the most stable KRas-Ligand complex (MD 1) is showed in Figure 3. As it can be seen, the system remains stable during the last 300 ns with an average value of ΔG binding = -27.4 kcal/mol for the last 20 ns. The complex starts at the p1 pocket with the three methoxide group inserted in the pocket and the fused rings exposed to the solvent. However, around 200 ns and during 50 ns the ligand changes its orientation doing a complete rotation to put the fused rings inside the p1 pocket and two of the methoxide group exposed to the solvent.

Also, for a better description of the behavior of the different complexes along the molecular dynamics progression, the $\Delta G_{binding}$ calculated using the MMGBSA methodology for each of the remaining seventeen complexes is reported in Figure S2 of the Supporting Information.

Residues of KRas that contribute to the binding free energy of the KRas-Ligand complex were analyzed during the last 20ns of the most stable molecular dynamics (MD 1). A 3D representation of the binding site and the interacting residues is showed in Figure 4 (3D structure in PDB format available as supporting information). Also, the averaged numerical values are reported in Figure S3 of the Supporting Information. From Figure 4 it can be seen that the ligand inserts in a deeper pocket where the fused rings interact with the hydrophobic residues Leu56, Glu63, Tyr64, Tyr71 and Thr74. However, the picture shows the possibility to increase the size of this ligand on the left of the pocket by modifications in the 1,4-dioxane group and in one of the methoxide groups. Also, the complex makes two stable hydrogen bonds (HB) with the protein (see Figure 4c). The first HB is established between the oxygen carbonyl of residue Glu37 and the NH of the isoquinoline nucleus. As it can be seen in Figure S4 of Supporting Information, this hydrogen bond is stable along the last 20 ns of MD (86.4% of occupation). The second hydrogen bond is formed between the OH of the ligand and both oxygens of the Glu37 residue. Figure S5 of Supporting Information shows the evolution of both distances along the time. We can see that this HB exists during the mayor part of the time (59.3% of occupation) but some time disappears. Thus, another hydrogen donor able to make stronger interactions with Glu37 should improve the ligand affinity. This fact can explain the better activity of compound **14** where the OH group is replaced by a NH_2 group.

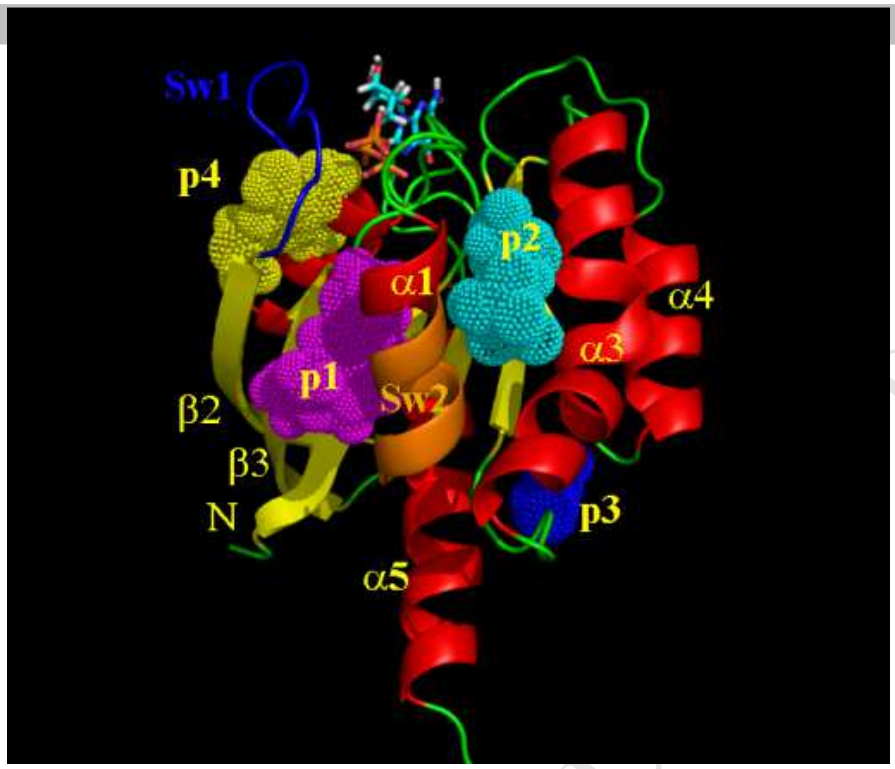

Figure 2. The most relevant structural motifs of the KRas protein are indicated. The functionally important switch regions Sw1 and Sw2 are highlighted in blue and orange respectively. The location of the four allosteric ligand-binding sites studied in this article is showed in colored mesh (p1 to p4). The GTP cofactor is represented in sticks.

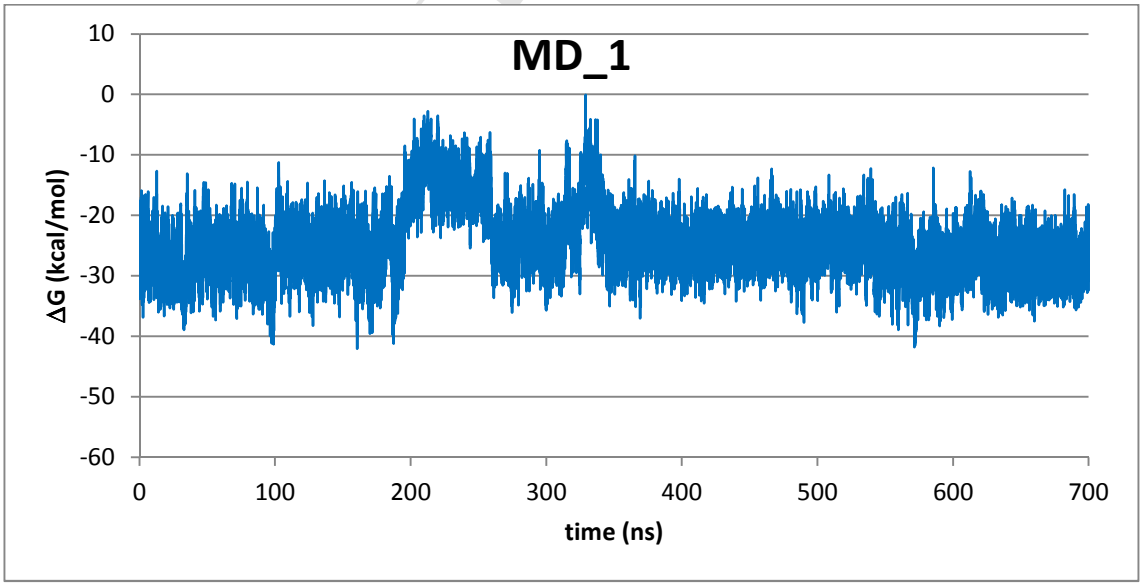

Figure 3. Evolution of $\Delta G_{binding}$ versus time for the most stable KRas-Ligand complex (MD_1) using the MMGBSA algorithm.

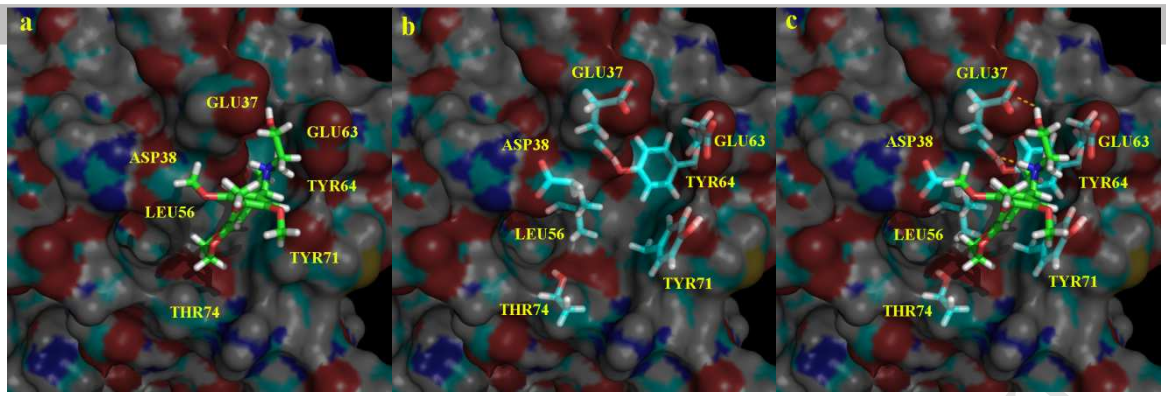

Figure 4. A Spatial representation of the complex KRas-Ligand for the most stable MD (MD_1). a) Description of the p1 pocket with the Ligand. b) Spatial representation of the most important residues that interact with the Ligand. c) The KRas-Ligand complex showing the hydrogen bonds in green. The 4DSN structure was used as starting point for the complexes.

4. Conclusion

In conclusion, the synthesis of substituted isoquinolines was accomplished through a process of aldehyde amination followed by cyclization and *N*-alkylation or *N*-arylation under classical conditions. The synthesized isoquinolines were tested for its biological activities. However, a rational design of novel compounds with increased inhibitory activity against KRas could be difficult without the knowledge of the binding site and therefore the interactions between the synthetized compounds and the KRas protein. In this sense, molecular modeling can help in obtaining important information and contributing to explain the *in vitro* results. The amine **14** and the alcohol **12** exhibit in vitro promising antileukemic activity (IC_{50} = 2.0 and 2.6 μM on L1210 cells respectively) and an investigation of cytotoxic mechanisms suggest the involvement of KRas inhibition in both without additional anti-angiogenic effects in the case of compound **12**.

5. Experimental section.

5.1. Chemistry

Melting points were obtained on an MFB-595010M Gallenkamp apparatus in open capillary tubes and are corrected. IR spectra were obtained using a FTIR Perkin-Elmer 1600 Infrared Spectrophotometer. Only noteworthy IR absorptions are listed (cm^{-1}). ^{1}H and ^{13}C NMR spectra were recorded on a Varian Gemini-200 (200 and 50.3 MHz respectively) or Varian Gemini-300 (300 and

75.5 MHz) or Varian Gemini-400 (400 and 100.6 MHz) Instrument using $CDCl_3$ as solvent with tetramethylsilane as internal standard or $(CD_3)_2CO$. Other ^1H NMR spectra and heterocorrelation ^1H-^{13}C (HMQC and HMBC) experiments were recorded on a Varian VXR-500 (500 MHz). Mass spectra were recorded on a Helwett-Packard 5988-A. Column chromatography was performed with silica gel (E. Merck, 70-230 mesh). Reactions were monitored by TLC using 0.25 mm silica gel F-254 (E. Merck). Microanalysis was determined on a Carlo Erba–1106 analyzer. All reagents were of commercial quality or were purified before use. Organic solvents were of analytical grade or were purified by standard procedures. Commercial products were obtained from Sigma-Aldrich. Elemental analysis was used to ascertained purity of >95% for all compounds of this work for which biological activities were determined.

5.1.1. ***(E)-6-(2-Nitrovinyl)-2,3-dihydro[1,4]benzodioxine (2).*** 2,3-Dihydro[1,4]benzodioxin-6-carbaldehyde **(1)** (1 g, 6.1 mmol) and ammonium acetate (123 mg, 1.57 mmol) were dissolved in nitromethane (10 mL) in a flame-dried round-bottom flask under argon and refluxed under stirring for 16 h. Then, TLC of the crude mixture (CH_2Cl_2 / hexane 7:3) indicated formation of a bright yellow compound (R_f = 0.55) and complete consumption of the starting material (R_f = 0.35). The crude mixture was filtered and concentrated *in vacuo* to afford *(E)*-6-(2-nitrovinyl)-2,3-dihydro[1,4]benzodioxine (**2**) (1.25 g, 99% yield) as a bright yellow solid. R_f = 0.55 (CH_2Cl_2/hexane 7:3). M.p. 148-150 ^oC (EtOAc). NMR ^1H ($CDCl_3$, 300 MHz) δ (ppm): 4.30 (s, 4H, C<u>H</u>$_2$-O (x 2)), 6.91 (d, *J* = 6.0 Hz, 1H, H-8), 7.05 (dd, *J* = 3.0 Hz, *J* = 6.0 Hz, 1H, H-7), 7.07 (d, *J* = 3.0 Hz, 1H, H-5), 7.47 (d, *J* = 13.5 Hz, 1H, C<u>H</u>=CH-NO_2), 7.90 (d, *J* = 13.5 Hz, 1H, CH=C<u>H</u>-NO_2). NMR ^{13}C ($CDCl_3$, 75.5 MHz) δ (ppm): 64.6 (CH_2 (x 2)), 117.7 (CH, C-5), 117.9 (CH, C-8), 122.0 (C, C-6), 122.0 (CH, C-7), 130.2 (CH, CH-NO_2), 142.7 (C, C-8a), 143.9 (C, C-4a), 151.1 (CH, CH=<u>C</u>H-NO_2).

5.1.2. **2-(2,3-Dihydro[1,4]benzodioxin-6-yl)ethylamine (3).** *(E)*-6-(2-Nitrovinyl)-2,3-dihydro[1,4]benzodioxine (**2**) (1.6 g, 7.68 mmol) was dissolved in EtOAc (80 mL) and MeOH (5 mL). 10% Palladium on charcoal catalyst (268 mg, 10% w/w) was added and the mixture was put under a 7 atm hydrogen atmosphere under stirring for 2 days. After 16 h, TLC of the crude mixture (hexane/EtOAc) indicated formation of a new compound and complete consumption of starting material (R_f = 0.80). The mixture was filtered and concentrated *in vacuo* to afford the phenethylamine **3** (852 mg, 53% yield as a brown oil. R_f = 0.55 (hexane/EtOAc 2:8). IR (film) ν cm^-

^{1}: 3100 (NH), 2910 (CH), 1200 (C-O). NMR ^{1}H ($CDCl_3$, 300 MHz) δ (ppm): 2.63 (t, *J* = 7.6 Hz, 2H, Ar-C<u>H</u>$_2$-CH$_2$), 2.91 (t, *J* = 7.6 Hz, 2H, CH$_2$-C<u>H</u>$_2$-NH$_2$), 4.24 (s, 4H, CH$_2$-O (x 2)), 6.66 (dd, *J* = 2 Hz, 8.2 Hz, 1H, H-7), 6.70 (d, *J* = 2 Hz, 1H, H-5), 6.80 (d, *J* = 8.2 Hz, 1H, H-8). NMR ^{13}C ($CDCl_3$, 75.5 MHz) δ (ppm): 38.7 (CH$_2$, CH$_2$-Ar), 43.1 (CH$_2$, CH$_2$-N), 63.8 (CH$_2$, CH$_2$-O), 63.9 (CH$_2$, CH$_2$-O), 116.7 (CH, C-5), 116.9 (CH, C-8), 121.2 (CH, C-7), 132.5 (C, C-6), 141.4 (C, C-4a), 142.9 (C, C-8a).

5.1.3. 2-(2,3-Dihydrobenzo[*b*][1,4]dioxin-6-yl)ethylamine (3). *(E)*-6-(2-Nitrovinyl)-2,3-dihydro[1,4]benzodioxine (**2**) (1 g, 4.82 mmol) was dissolved in THF (20 mL). $LiAlH_4$ (740 mg, 19.5 mmol) was added portion wise. The reaction was stirred at rt for 20 h and TLC of the reaction mixture (hexane/EtOAc 1:1) indicated formation of a new compound and complete consumption of starting material (R_f = 0.60). The crude mixture was quenched dropwise with water (1 mL) and filtered. The solid residue was extracted with CH_2Cl_2 (3 x 20 mL) and the combined organic phases were dried (Na_2SO_4), filtered and concentrated *in vacuo* to afford 2-(2,3-dihydro[1,4]benzodioxin-6-yl)ethylamine (**3**) (530 mg, 61% yield) as a pale brown oil. This material was identical in all respects with that previously described.

5.1.4. 2-(2,3-Dihydro[1,4]benzodioxin-6-yl)ethylamine (3). 6-(2-benzylamineethyl)-2,3-dihydro benzo[1,4]dioxine (200 mg, 1.01 mmol) was dissolved in EtOAc (80 mL) and MeOH (5 mL). 10% Palladium on charcoal catalyst (268 mg) and HCl (30 µL) were added and the mixture was put under hydrogen atmosphere under stirring for 2 days. The crude mixture was concentrated *in vacuo*. The residue was purified by silica gel flash column chromatography to afford 2-(2,3-dihydro[1,4]benzodioxin-6-yl)ethylamine (**3**) (71 mg, 53% yield) as a brown oil. Analytical data was identical with the previously described compound.

5.1.5. (6-(3,4,5-Trimethoxyphenyl)-2,3,6,7,8,9-hexahydro-[1,4]dioxino[2,3-*g*]isoquinolin-7-yl) 2,2,2-trifluoroacetate (6). To a solution of 2-(2,3-dihydrobenzo[*b*][1,4]dioxin-6-yl)ethylamine **3** (250 mg, 1.39 mmol) in ethanol (20 mL) was added HCl (0.1 mL), molecular sieves (50 mg) and 3,4,5-trimethoxybenzaldehyde **4** (410 mg, 2.09 mmol) in a flame-dried round-bottom flask under argon. Et_3N was added until p*H* 6-6.5 was reached and the mixture was heated to reflux under stirring for 16 h. The mixture was concentrated *in vacuo* and the residue was dissolved in EtOAc (20 mL), washed with NaOH (3 x 20 mL of a 2N solution), dried (Na_2SO_4), filtered and concentrated *in*

vacuo to afford brown oil. CF_3COOH (3 mL, excess amount) and $(CF_3CO)_2O$ (3 mL, excess amount) were added and the crude mixture was refluxed under stirring for 16 h. Then, TLC of the crude mixture (EtOAc/hexane 1:1) indicated presence of a new compound (R_f = 0.75) and uncomplete consumption of the 3,4,5-trimethoxybenzaldehyde (R_f = 0.80). The mixture was dissolved in EtOAc (20 mL), washed with NaOH (3 x 30 mL of a 2N solution), dried (Na_2SO_4) filtered and concentrated *in vacuo*. The crude residue was purified by silica gel flash column chromatography (hexane/EtOAc 7:3) to afford the desired isoquinoline **6** (102 mg, 16% yield) as a brown oil. R_f = 0.75 (hexane/EtOAc 1:1). IR (film) ν cm^{-1}: 1686 (C=O), 1504 (Ar-H), 1299 (Ar-O), 1127 (C-O). NMR ^1H ($CDCl_3$, 300 MHz) δ (ppm): 2.75-2.82 (m, 1H, C<u>H</u>$_2$-CH_2-N), 2.94-3.05 (m, 2H, CH_2-C<u>H</u>$_2$-N, C<u>H</u>$_2$-CH_2-N), 3.18-3.25, (m, 1H, CH_2-C<u>H</u>$_2$-N), 3.77 (s, 6H, CH_3-O (x 2)), 3.83 (s, 3H, CH_3-O), 4.20-4.25 (m, 4H, CH_2-O), 6.45 (s, 2H, H-2', H-6'), 6.57 (s, 1H, H-5), 6.62 (s, 1H, H-6), 6.70 (s, 1H, H-10). NMR ^{13}C ($CDCl_3$, 75.5 MHz) δ (ppm): 28.4 (CH_2, CH_2N), 39.5 (CH_2, CH_2-Ar), 56.2 (CH, C-6), 60.8 (CH_3, OCH_3 (x 2)), 64.4 (CH_3, OCH_3), 64.6 (CH_2, CH_2-O(x 2)), 106.2 (CH, C-2', C-6'), 116.5 (CH, C-5), 116.3 (C, *J* = 288 Hz, CF_3), 116.8 (CH, C-10), 126.0 (C, C-1'), 136.5 (C, C-5a), 137.8 (C, C-9a), 142.3 (C, C-10a), 142.9 (C, C-4a), 152.9 (C, C-4'), 153.0 (C, C-3', C-5'), 156.4 (C, C=O). MS (EI) (m/z, %): 453 (M^+, 71), 438 (M^+-CH_3, 100), 286 (M^+-$C_9H_{11}O_3$, 32). ($C_9H_{11}O_3$ = 3,4,5-trimethoxyphenyl. MS EI m/z (%): 453 (M^+, 12), 355 (M^+-C_2F_3O, 100).

5.1.6. 6-(3,4,5-Trimethoxyphenyl)-2,3,6,7,8,9-hexahydro[1,4]dioxino[2,3-*g*]isoquinoline (8). The isoquinolin-trifluoroacetate **6** (285 mg, 0.63 mmol) was dissolved in MeOH (15 mL), then NaOH 2N (45 mL) was added and the reaction was heated to reflux overnight under stirring. Then, TLC of the crude mixture (EtOAc/hexane 1:1) showed total consumption of SM (R_f = 0.80) and formation of the desired product (R_f = 0.10). The methanol was evaporated *in vacuo* and the aqueous phase was extracted with diethyl ether (3 x 20 mL). The combined organic phases were dried (Na_2SO_4), filtered and concentrated *in vacuo* to afford the substituted isoquinoline **8** (218 mg, 97% yield) as a brown solid. R_f = 0.30 (EtOAc). M.p. 131-132 ^oC (diethyl ether). IR (KBr) ν cm^{-1}: 3100 (NH), 1589 (C=C), 1297 (Ar-O), 1125 (C-O). RMN ^1H ($CDCl_3$, 300 MHz) δ (ppm): 2.54-2.65 (m, 1H, C<u>H</u>$_2$-CH_2-N), 2.83-3.03 (m, 2H, CH_2-C<u>H</u>$_2$-N, C<u>H</u>$_2$-CH_2-N), 3.18-3.25 (m, 1H, CH_2-C<u>H</u>$_2$-N), 3.75 (s, 6H, CH_3-O (x 2)), 3.77 (s, 3H, CH_3-O), 4.13 (m, 4H, CH_2-O (x 2)), 4.81 (s, 1H, H-6), 6.22 (s, 1H, H-5), 6.45 (s,

2H, H-2', H-6'), 6.56 (s, 1H, H-10). RMN ^{13}C ($CDCl_3$, 75.5 MHz) δ (ppm): 28.9 (CH_2, C-9), 43.1 (CH_2, CH_2N), 56.0 (CH_3, OCH_3 (x 2)), 60.7 (CH_3, OCH_3), 62.4 (CH, C-6), 64.3 (CH_2, OCH_2), 64.2 (CH_2, OCH_2), 105.6 (CH, C-2', C-6'), 115.9 (CH, C-5), 116.6 (CH, C-10), 128.1 (C, C-5a), 131.3 (C, C-9a), 140.1 (C, C-1'), 141.4 (C, C-4a), 141.9 (C, C-10a), 152.8 (C, C-4'), 152.9 (C, C-3', C-5'). HRMS ESI(+) m/z for $C_{20}H_{24}NO_5$ $[M+H]^+$ calcd. 358.1654, found: 358.1651.

5.1.7. 6-(3,4,5-Trimethoxyphenyl)-2,3,6,7,8,9-hexahydro[1,4]dioxino[2,3-*g*]isoquinoline (8) (alternative synthesis). The phenethylamine **3** (228 mg, 0.84 mmol) and 3,4,5-trimethoxybenzaldehyde (**4**) (274 mg, 0.92 mmol) were dissolved in benzene (15 mL) in a flame-dried round-bottom flask under argon. The reaction mixture was heated to reflux under stirring in a Dean Stark reaction for 4 h. The solution was cooled at 0 ^oC and H_3PO_4 (2 mL of 85% aqueous solution) was added. The reaction mixture was refluxed under stirring in a Dean Stark reaction for 3 h and TLC of the crude mixture (EtOAc) indicated presence of the tetrahydroisoquinoline desired product (R_f 0.30) and uncomplete consumption of the aldehyde (R_f = 0.80). The reaction mixture was cooled at 0 ^oC and quenched with NaOH (5 mL of a 2N aqueous solution). Then the mixture was dissolved in CH_2Cl_2 (20 mL), washed with NaOH 2N (3 x 30 mL) and the organic phases were re-extracted with CH_2Cl_2 (3 x 20 mL). The combined organic phases were dried (Na_2SO_4), filtered and concentrated *in vacuo*. The residue was purified by silica gel flash column chromatography (hexane/EtOAc 3:7) to afford the tetrahydroisoquinoline **8** (200 mg, 40% yield) as a brown solid. The reaction was scaled up using 2 g of phenethylamine **3** to afford **8** (2.4 g, 55% yield) as a brown solid. Analytical data was identical with the previously described compound.

5.1.8. 6-(3,4,5-Trimethoxyphenyl)-2,3-dihyhydro[1,4]dioxino[2,3-*g*]isoquinoline (10). 6-(3,4,5-Trimethoxyphenyl)-2,3,6,7,8,9-hexahydro[1,4]dioxino[2,3-*g*]isoquinoline (**8**) was oxidized to isoquinoline **10** using Pd/C in decahydronaphthalene [8a].

5.1.9. General *N*-alkylation procedure to tetrahydroquinolines. The tetrahydroisoquinoline (150 mg, 0.42 mmol) was dissolved in DMF (7 mL) and put in a flame-dried round-bottom flask under argon. The alkylating agent (0.11 mL, 1.66 mmol), KI (cat) and Et_3N (0.47 mL, 3.36 mmol) were added under argon. The reaction was stirred at rt and the corresponding alkylating agent (0.11 mL, 1.66 mmol) and KI (cat) were added every day under argon for 7 days. Water (20 mL) was added and the crude mixture was extracted with diethyl ether (3 x 20 mL). The combined organic phases were

washed with H_2O (5 x 30 mL), dried (Na_2SO_4), filtered and concentrated *in vacuo.* The crude residue was purified by silica gel flash column chromatography to afford the corresponding isoquinoline.

5.1.10. 7-Etoxycarbonil-2-[6-(3,4,5-trimethoxyphenyl)-2,3,6,7,8,9-hexahydro[1,4]dioxino[2,3-*g*] isoquinoline (11). From the tetrahydroisoquinoline **8** (55 mg, 0.15 mmol) and ethyl chloroformate (0.05 mL, 0.23 mmol, d 1.125), and following the general procedure described above the title compound was obtained (53 mg, 79% yield) as yellow oil. R_f = 0.52 (EtOAc/Hex 5:5). IR (film) ν cm^{-1}: 1856-1920 (C-H), 1654, 1502, 1465, 1222 (Ar-0), 1082 (Ar-O). NMR ^1H ($CDCl_3$, 200 MHz) δ (ppm): 1.28 (t, *J* = 7Hz, 3H, CH_3), 2.60-2.85 (m, 2H, H-9), 3.13-3.27 (m, 2H, H-8), 3.79 (s, 6H, CH_3-O (x 2)), 3.80 (s, 3H, CH_3-O), 4.19 (q, *J* = 7 Hz, 4H, CH_2-O), 4.36 (s, 1H, H-1), 6.43 (s, 2H, H-2', H-6'), 6.54 (s, 1H, H-10), 6.66 (s, 1H, H-5). NMR ^{13}C ($CDCl_3$, 50.4 MHz) δ (ppm): 14.8 (CH_3), 27.8 (CH_2), 38.2 (CH_2), 56.1 (CH_3-O x 2), 57.1 (CH), 60.6 (CH_3-O), 61.5 (CH_2-O), 64.3 and 64.4 (CH2-O x 2), 105.6 (C-2'and C-6'), 116.6 (C-5 and C-10), 127.9 (C-9a), 137.1 (C-5a, C-4'), 138.5 (C-1'), 141.8 (C-4a), 142.5 (C-10a), 152.8 (C-3'and C-5'), 155.3 (CO). HRMS ESI(+) m/z for $C_{23}H_{28}NO_7$ $[M+H]^+$ calcd. 430.1866, found: 430.1854.

5.1.11. 2-[6-(3,4,5-Trimethoxyphenyl)-2,3,6,7,8,9-hexahydro[1,4]dioxino[2,3-*g*]isoquinolin-7-yl)] ethanol (12). From the tetrahydroisoquinoline **8** (150 mg, 0.42 mmol) and 2-chloroethanol (0.11 mL, 1.66 mmol), and following the general procedure described above the title compound was obtained (54 mg, 32% yield) as a white solid. R_f = 0.50 (EtOAc/MeOH 9:1). M.p. 120-122 ^oC (CH_2Cl_2). IR (film) ν cm^{-1}: 3527 (OH), 1852-1920 (C-H), 1593, 1502, 1465, 1422 (Ar-H), 1302, 1127 (Ar-O), 1062 (Ar-O). NMR ^1H ($CDCl_3$, 300 MHz) δ (ppm): 2.36-2.43 (m, 1H, Ar-C$\underline{H}_2$-CH_2-N), 2.52-2.61 (m, 1H, Ar-C$\underline{H}_2$-CH_2-N), 2.71-2.85 (m, 2H, N-C$\underline{H}_2$-CH_2-OH), 2.95-3.05 (m, 1H, Ar-CH_2-C$\underline{H}_2$-N), 3.21-3.28 (m, 1H, Ar-CH_2-C$\underline{H}_2$-N), 3.40-3.47 (m, 1H, C$\underline{H}_2$-OH), 3.65-3.73 (m, 1H, C$\underline{H}_2$-OH), 3.81 (s, 6H, CH_3-O (x 2)), 3.84 (s, 3H, CH_3-O), 4.15-4.25 (m, 4H, O-CH_2-CH_2-O), 4.40 (s, 1H, H-6), 6.26 (s, 1H, H-5), 6.45 (s, 2H, H-2', H-6'), 6.63 (s, 1H, H-10). NMR ^{13}C ($CDCl_3$, 75.5 MHz) δ (ppm): 28.6 (CH_2, Ar-$\underline{C}H_2$-CH_2-N). 47.8 (CH_2, Ar-CH_2-$\underline{C}H_2$-N), 55.6 (CH_2, N-$\underline{C}H_2$-CH_2-OH), 56.5 (CH_3, CH_3-O (x 2)), 58.5 (CH_2, Ar-CH_2-$\underline{C}H_2$-OH), 61.2 (CH_3, CH_3-O), 64.7 (CH_2, O-CH_2-$\underline{C}H_2$-O), 64.7 (CH_2, O-$\underline{C}H_2$-CH_2-O), 69.4 (CH, C-6), 106.7 (CH, C-2', C-6'), 116.4 (CH, C-5), 117.1 (CH, C-10), 127.7 (C, C-5a), 131.3 (C, C-9a), 139.6 (C, C-1'), 141.9 (C, C-4a), 142.4 (C, C-10a), 153.5 (C, C-3',

C-4', C-5'). MS (EI) (m/z, %): 401 (M^+, 6), 370 (M^+-CH_2OH, 100), 234 (M^+-$C_9H_{12}O_3$, 78). ($C_9H_{11}O_3$ = 3,4,5-trimethoxyphenyl). HRMS ESI(+) m/z for $C_{22}H_{28}NO_6$ $[M+H]^+$ calcd. 402.1917, found: 402.1912.

5.1.12. 2-(6-(3,4,5-Trimethoxyphenyl)-2,3,6,7,8,9-hexahydro[1,4]dioxino[2,3-*g*]isoquinolin-7-yl) acetonitrile (13). From the tetrahydroisoquinoline **8** (150 mg, 0.42 mmol) and chloroacetonitrile (0.08 mL, 1.26 mmol), and following the general procedure described above the title compound was obtained (140 mg, 84% yield) as a brown solid. R_f = 0.85 (EtOAc). M.p. 144-146 ^oC (hexane/EtOAc). IR (film) ν cm^{-1}: 2925 (C-H), 2363 (CN), 1588, 1503, 1455, 1417 (Ar-H), 1295, 1233 (Ar-O), 1122, 1066 (C-O). NMR ^1H ($CDCl_3$, 300 MHz) δ (ppm): 2.65-2.75 (m, 1H, Ar-C$\underline{H}_2$-CH_2-N), 2.85-3.00 (m, 1H, Ar-C$\underline{H}_2$-CH_2-N), 3.01-3.35 (m, 2H, Ar-CH_2-C$\underline{H}_2$-N), 3.43 (s, 2H, C$\underline{H}_2$-CN), 3.80 (s, 6H, OCH_3 (x 2)), 3.82 (s, 3H, OCH_3), 4.09-4-26 (m, 4H, O-CH_2-CH_2-O), 4.45 (s, 1H, H-6), 6.18 (s, 1H, H-5), 6.52 (s, 2H, H-2', H-6'), 6.58 (s, 1H, H-10). NMR ^{13}C ($CDCl_3$, 75.5 MHz) δ (ppm): 29.0 (CH_2, Ar-$\underline{C}H_2$-CH_2-N), 44.3 (CH_2, CH_2-N), 50.5 (Ar-$\underline{C}H_2$-CN), 56.5 (CH_3, CH_3-O (x 2)), 61.1 (CH_3, CH_3-O), 64.6 (CH_2, O-CH_2-$\underline{C}H_2$-O), 64.7 (CH_2, O-$\underline{C}H_2$-CH_2-O), 67.6 (CH, C-6), 106.3 (CH, C-2', C-6'), 115.1 (C, CN), 116.4 (CH, C-5), 116.9 (CH, C-10), 126.8 (C, C-5a), 130.7 (C, C-9a), 137.7 (C, C-1'), 137.9 (C, C-1'), 142.0 (C, C-4a), 142.5 (C, C-10a), 153.4 (C, C-4'), 153.8 (C, C-3', C-5'). MS (EI) (m/z, %): 396 (M^+, 33), 229 (M^+-$C_9H_{12}O_3$, 100). ($C_9H_{11}O_3$ = 3,4,5-trimethoxyphenyl). HRMS ESI(+) m/z for $C_{22}H_{25}NO_5$ [M+H]+ calcd. 397.1763, found: 397.1764

5.1.8. 2-(6-(3,4,5-Trimethoxyphenyl)-2,3,6,7,8,9-hexahydro[1,4]dioxino[2,3-*g*]isoquinolin-7-yl) ethylamine (14). The isoquinoline **13** (115 mg, 0.29 mmol) was dissolved in THF (10 mL) in a flame-dried round-bottom flask under argon, and $LiAlH_4$ (35 mg, 0.86 mmol) was added. The reaction was stirred at rt for 16 h and TLC of the crude mixture (EtOAc/MeOH, 7:3) showed formation of a new compound (R_f = 0.25) and complete consumption of SM (0.95). The crude mixture was quenched dropwise with water and filtered. The solid residue was extracted with CH_2Cl_2 (3 x 20 mL) and the combined organic phases were dried (Na_2SO_4), filtered and concentrated *in vacuo*. The residue was purified by silica gel flash column chromatography (EtOAc/MeOH, 2:8) to afford the isoquinoline **14** (60 mg, 52% yield) as a yellow solid. R_f = 0.25 (EtOAc/MeOH 7:3). M.p. 55-60 °C (hexane/EtOAc). IR (film) ν cm^{-1}: 3300-3100 (NH_2), 2923, 2834 (C-H), 1588, 1503, 1456, 1418 (Ar-H), 1296, 1232 (Ar-O) 1122, 1066 (C-O). NMR ^1H ($CDCl_3$, 300 MHz) δ (ppm): 2.40-2.56

(m, 2H, CH_2-Ar), 2.59-2.85 (m, 4H, CH_2-N (x 2), 2.96-3.06 (m, 1H, C$\underline{H}_2$-N), 3.15-3.22 (m, 1H, C$\underline{H}_2$-N), 3.81 (s, 6H, CH_3-O (x 2)), 3.84 (s, 3H, CH_3-O), 4.14-4.20 (m, 4H, O-CH_2-CH_2-O), 4.27 (s, 1H, H-6), 6.25 (s, 1H, H-5), 6.51 (s, 2H, H-2', H-6'), 6.61 (s, 1H, H-10). NMR ^{13}C ($CDCl_3$, 75.5 MHz) δ (ppm): 28.9 (CH_2, Ar-$\underline{C}H_2$-CH_2-N), 39.4 (CH_2, N-CH_2-$\underline{C}H_2$-NH_2), 48.4 (CH_2, Ar-CH_2-$\underline{C}H_2$-N), 56.4 (CH_3, OCH_3 (x 2)), 57.4 (CH_2, 2H, N-$\underline{C}H_2$-CH_2-NH_2) , 61.1 (CH_3, OCH_3), 64.6 (CH_2, O-CH_2-$\underline{C}H_2$-O), 64.7 (CH_2, O-$\underline{C}H_2$-CH_2-O), 69.9 (CH, C-6), 106.7 (CH, C-2', C-6'), 116.4 (CH, C-5), 117.0 (CH, C-10) , 127.9 (C, C-5a), 131.8 (C, C-9a), 140.2 (C, C-1'), 141.8 (C, C-4a), 142.2 (C, C-10a), 153.4 (C, C-3', C-4', C-5'). MS EI m/z (%): 400 (M^+, 1), 370 (M^+-CH_5N, 64) 355 (M^+-C_2H_7N, 57). HRMS ESI(+) m/z for $C_{22}H_{29}N_2O_5$ $[M+H]^+$ calcd. 401.2076, found: 401.2082.

5.1.9. *N,N*-Dimethyl-(6-(3,4,5-trimethoxyphenyl)-2,3,6,7,8,9-hexahydro[1,4]dioxino[2,3-*g*]isoquino lin-7-yl))ethylamine (15). From the tetrahydroisoquinoline **8** (100 mg, 0.28 mmol) and 2-dimethylaminoethyl chloride (121 mg, 0.84 mmol), and following the general procedure described above the title compound was obtained (67 mg, 54% yield) as a yellow oil. R_f = 0.25 (EtOAc/MeOH 8:2). IR (film) ν cm^{-1}: 2935, 2800 (C-H), 1589, 1505, 1418 (Ar-H), 1290, 1235, 1124 (Ar-O), 1067 (C-O). NMR ^{1}H ($CDCl_3$, 300 MHz) δ (ppm): 2.31 (s, 6H, CH_3-N (x 2)), 2.64 (t, *J* = 6 Hz, 2H, N-CH_2-CH_2-N), 2.69 (t, *J* = 6 Hz, 2H, N-CH_2-CH_2-N), 2.80-2.95 (m, 2H, Ar-C$\underline{H}_2$-CH_2-N), 3.20-3.29 (m, 2H, Ar-CH_2-C$\underline{H}_2$-N), 3.78 (s, 6H, OCH_3 (x 2)), 3.82 (s, 3H, OCH_3), 4.20-4.30 (m, 4H, O-CH_2-CH_2-O), 4.28 (s, 1H, H-6), 6.45 (s, 2H, H-2', H-6'), 6.57 (s, 1H, H-5), 6.68 (s, 1H, H-10). NMR ^{13}C ($CDCl_3$, 75.5 MHz) δ (ppm): 38.7 (CH_3, CH_3-N x 2), 46.1 (CH_2, Ar-CH_2), 56.5 (CH_2, N-CH_2), 57.73 (CH, C-6), 57.8 (CH_3, O-CH_3), 58.5 (CH_2, N-CH_2), 61.2 (CH_3, OCH_3 (x 2)), 63.8 (CH_2, N-CH_2), 64.7 (CH_2, O-CH_2-), 64.8 (CH_2, CH_2-O), 106.1 (CH, C-2', C-6'), 116.9 (CH, C-5), 117.1 (CH, C-10), 128.4 (C, C-5a), 137.7 (C, C-9a), 138.8 (C, C-1') 142.2 (C, C-4a), 142.9 (C, C-10a), 153.2 (C, C-3', C-4', C-5'). MS (EI) (m/z, %): 428 (M^+, 21). HRMS ESI(+) m/z for $C_{24}H_{33}N_2O_5$ $[M+H]^+$ calcd. 429.2389, found: 429.2385.

5.1.10. *N,N*-Diethyl-(6-(3,4,5-trimethoxyphenyl)-2,3,6,7,8,9-hexahydro[1,4]dioxino[2,3-*g*] isoquinolin-7-yl))ethylamine (16). From the tetrahydroisoquinoline **8** (53 mg, 0.14 mmol) and 2-dietilaminoethyl chloride (51 mg, 0.28 mmol), and following the general procedure described above the title compound was obtained (16 mg, 25% yield) as a yellow oil. R_f = 0.27 (EtOAc/MeOH 8:2). IR (film) ν cm^{-1}: 2939, 2812 (C-H), 1586, 1500, 1186 (Ar-O), 1098 (C-O). NMR ^{1}H ($CDCl_3$, 200

MHz) δ (ppm): 0.94 (t, *J* = 7 Hz, 6H, CH_3- x 2), 1.98-2.04 (m, 4H, CH_2 x2), 2.45 (q, *J* = 7Hz, 4H, N-CH_2 x2), 2.67 (t, *J* = 7 Hz, 2H, N-CH_2), 2.82-2.95 (m, 2H, Ar-CH_2), 3.21-3.28 (m, 2H, Ar-CH_2), 3.82 (s, 6H, OCH_3 (x 2)), 3.83 (s, 3H, OCH_3), 4.18-4-19 (m, 4H, O-CH_2-CH_2-O), 4.29 (s, 1H, H-6), 6.22 (s, 1H, H-5), 6.53 (s, 2H, H-2', H-6'), 6.62 (s, 1H, H-10). NMR ^{13}C ($CDCl_3$, 50.4 MHz) δ (ppm): 11.2 (CH_3, CH_3-N (x 2)), 28.7 (CH_2, Ar-CH_2), 47.2 (CH_2, N-CH_2 x 2), 49.3 (CH_2, N-CH_2), 50.3 (CH_2, N-CH_2), 51.9 (CH_2, N-CH_2), 56.1 (CH_3, OCH_3 (x 2)), 60.9 (CH_3, O-CH_3), 64.3 (CH_2, O-CH_2-), 64.4 (CH_2, -CH_2-O), 69.6 (CH-Ar), 106.2 (CH, C-2', C-6'), 116.0 (CH, C-5), 116.6 (CH, C-10), 122.1 (C, C-9a), 127.5 (C, C-5a), 130.3 (C-1'), 139.8 (C-4'), 141.3 (C-10a), 141.8 (C-4a), 152.9 (C-3', C-5'). HRMS ESI(+) m/z for $C_{26}H_{37}N_2O_5$ $[M+H]^+$ calcd. 457.2702, found: 457.2712.

5.1.11. Ethyl 6-(6-(3,4,5-trimethoxyphenyl)-2,3,8,9-tetrahydro-[1,4]dioxino[2,3-*g*]isoquinolin-7(6*H*)-yl)hexanoate (17). From the tetrahydroisoquinoline **8** (100 mg, 0.27 mmol) and methyl 6-bromohexanoate (87 mg, 0.41 mmol), and following the general procedure described above the title compound was obtained (62 mg, 46% yield) as a yellow oil. R_f = 0.40 (EtOAc/hexane 8:2). IR (film) ν cm^{-1}: 2938, 1736, 1589, 1512, 1298 (Ar-O), 1125 (C-O). NMR ^{1}H ($CDCl_3$, 300 MHz) δ (ppm): 1.43-1.58 (m, 9H, CH_2- x 3 and CH_3-), 2.14-2.26 (m, 2H, CH_2-CO), 2.40-2.42 (m, 2H, CH_2-N), 2.67-2.75 (m, 1H, N-CH_2), 2.80-2.96 (m, 2H, Ar-CH_2), 3.21-3.28 (m, 1H, -CH_2), 3.82 (s, 6H, OCH_3 (x 2)), 3.83 (s, 3H, OCH_3), 4.18-4-19 (m, 6H, O-CH_2-CH_2-O and CH_2-O), 4.29 (s, 1H, H-6), 6.25 (s, 1H, H-5), 6.51 (s, 2H, H-2', H-6'), 6.61 (s, 1H, H-10). NMR ^{13}C ($CDCl_3$, 50.4 MHz) δ (ppm): 24.9 (CH_2), 26.4 (CH_2), 26.9 (CH_2), 28.6 (CH_2), 34.0 (CH_2-COO-), 48.0 (CH_2), 51.2 (CH, N-CH), 54.2 (CH_2, N-CH_2), 56.0 (CH_3, OCH_3 (x 2)), 60.8 (CH_3, O-CH_3), 64.3 (CH_2, O-CH_2-), 64.4 (CH_2, -CH_2-O), 69.3 (CH-Ar), 106.1 (CH, C-2', C-6'), 116.0 (CH, C-5), 116.6 (CH, C-10), 124.7 (C, C-9a), 127.7 (C, C-5a), 131.7 (C-1'), 139.9 (C-4'), 141.2 (C-10a), 141.6 (C-4a), 152.8 (C-3', C-5'), 174.0 (C=O). HRMS ESI(+) m/z for $C_{28}H_{38}NO_7$ $[M+H]^+$ calcd. 500.2648, found: 500.2646.

5.1.12. 6-(6-(3,4,5-Trimethoxyphenyl)-2,3,8,9-tetrahydro-[1,4]dioxino[2,3-*g*]isoquinolin-7(6*H*)-yl)hexanoic acid (18). The tetrahydroisoquinoline **17** (40 mg, 0.82 mmol) was disolved in 2N NaOH solution (10 mL). The reaction mixture was vigorously stirred at room temperature for 6 h and TLC of the crude reaction (hexane/EtOAc 5:5) indicated formation of a new compound (R_f = 0.1). HCl 2N (15 mL) was added to the crude of reaction, and the mixture was extracted with EtOAc (2 x 10 mL). The organic fraction was dried over Na_2SO_4. After concentration the resulting yellowish solid

was purified by silica gel column chromatography using EtOAc/MeOH as eluent and the carboxylic acid was obtained (32 mg, 85% yield) as white solid. R_f = 0.1 (EtOAc/hexane 8:2). M.p. 63-64 ºC. IR (film) ν cm^{-1}: 2928, 1725, 1589, 1504, 1299 (Ar-O), 1126 (C-O). NMR ^{1}H ($CDCl_3$, 200 MHz) δ (ppm): 1.15-1.25 (m, 2H, CH_2-), 1.51-1.58 (m, 4H, CH_2-), 2.24 (t, *J* = 7 Hz, 2H, CH_2-), 2.44-2.47 (m, 2H, N-CH_2), 2.80-2.83 (m, 1H, CH_2), 2.97-3.08 (m, 2H, -CH_2), 3.22-3.31 (m, 1H, CH_2), 3.80 (s, 6H, OCH_3 (x 2)), 3.84 (s, 3H, OCH_3), 4.18-4-19 (m, 4H, O-CH_2-CH_2-O), 4.41 (s, 1H, H-6), 6.26 (s, 1H, H-5), 6.51 (s, 2H, H-2', H-6'), 6.61 (s, 1H, H-10). NMR ^{13}C ($CDCl_3$, 50.4 MHz) δ (ppm): 24.9 (CH_2), 25.5 (CH_2), 26.9 (CH_2), 27.4 (CH_2), 29.7 (CH_2), 46.9 (CH_2-COO-), 53.8 (CH_2), 56.1 (CH_3, OCH_3 (x 2)), 60.9 (CH_3, O-CH_3), 64.3 (CH_2, O-CH_2-), 64.4 (CH_2, -CH_2-O), 68.4 (CH-Ar), 106.6 (CH, C-2', C-6'), 116.1 (CH, C-5), 116.7 (CH, C-10), 127.1 (C, C-9a), 130.1 (C, C-5a), 137.0 (C-1'), 138.0 (C-4'), 141.5 (C-10a), 142.0 (C-4a), 152.9 (C-3', C-5'), 178.1 (C=O). HRMS ESI(+) m/z for $C_{26}H_{34}NO_7$ $[M+H]^+$ calcd. 472.2335, found: 472.2353.

5.1.13. *N*-(3,3-(Diethoxy)propyl)-6-(3,4,5-trimethoxyphenyl)-2,3,6,7,8,9-hexahydro[1,4]dioxino [2,3-*g*]isoquinoline (19). From the tetrahydroisoquinoline **8** (200 mg, 0.56 mmol) and 3-chloropropionaldehydediethyl acetal (0.14 mL, 0.84 mmol), and following the general procedure described above the title compound was obtained (80 mg, 30% yield) as a white oil. R_f = 0.80 (EtOAc). IR (film) ν cm^{-1}: 2949, 2929 (C-H), 1586, 1505, 1457 (Ar-H), 1300, 1122 (Ar-O), 1062 (C-O). NMR ^{1}H ($CDCl_3$, 300 MHz) δ (ppm): 1.05 (t, *J* = 6.9 Hz, 3H, O-CH_2-C$\underline{H}_3$), 1.13 (t, *J* = 6.9 Hz, 3H, O-CH_2-C$\underline{H}_3$), 1.70-1.85 (m, 2H, N-CH_2-C$\underline{H}_2$-CH), 2.20-2.35 (m, 1H, Ar-C$\underline{H}_2$-CH_2-N), 2.40-2.80 (m, 6H, Ar-C$\underline{H}_2$-C$\underline{H}_2$-N, N-C$\underline{H}_2$-CH_2-CH), 2.90-3.10 (m, 2H, Ar-CH_2-C$\underline{H}_2$-N), 3.14-3.33 (m, 2H, O-C$\underline{H}_2$-CH_3), 3.37-3.60 (m, 2H, O-C$\underline{H}_2$-CH_3), 3.81 (s, 6H, OCH_3 (x 2)), 3.83 (s, 3H, OCH_3), 4.12-4.22 (m, 4H, O-CH_2-CH_2-O), 4.26 (s, 1H, H-6), 4.45 (t, *J* = 5.1 Hz, 1H, CH_2-CH_2-C$\underline{H}$), 6.24 (s, 1H, H-5), 6.51 (s, 2H, H-2', H-6'), 6.59 (s, 1H, H-10). NMR ^{13}C ($CDCl_3$, 75.5 MHz) δ (ppm): 25.9 (CH_3, OCH_3), 28.9 (CH_3, O-CH_2-CH_3), 31.2, (CH_2, $\underline{C}H_2$-CH), 48.6 (CH_2, Ar-$\underline{C}H_2$), 50.5 (CH_2, Ar-CH_2-$\underline{C}H_2$-N), 56.4 (CH_3, OCH_3 (x 2)), 57.2 (CH_3, OCH_3), 60.7 (CH_2, N-$\underline{C}H_2$-CH_2-CH), 61.1 (CH_2, O-CH_2-CH_3), 61.6 (CH_2, CH_3-$\underline{C}H_2$-O), 63.1 (CH_2, O-CH_2-$\underline{C}H_2$-O), 64.7 (CH_2, O-$\underline{C}H_2$-CH_2-O), 69.4 (CH, C-6), 101.7 (CH, CHOO), 106.7 (CH, C-2', C-6'), 116.3 (CH, C-5), 116.5 (CH, C-10), 127.9 (C-5a), 132.9 (C-4a), 137.3 (C-1'), 141.7 (C, C-9a), 142.1 (C, C-10a), 153.3 (C, C-3', C-5'), 153.9

(C, C-4'). MS (EI) (m/z, %): 487 (M^+, 4), 370 (M^+-$C_7H_{16}O_2$, 65), 356 (M^+-$C_6H_{14}O_2$], 94) 320 (M-$C_9H_{12}O_3$, 100). ($C_9H_{11}O_3$ = 3,4,5-trimethoxyphenyl). HRMS ESI(+) m/z for $C_{27}H_{38}NO_7$ $[M+H]^+$ calcd. 488.2648, found: 488.2645.

5.1.14. *N*-(4-Nitrophenyl)-6-(3,4,5-trimethoxyphenyl)-2,3,6,7,8,9-hexahydro[1,4]dioxino[2,3-*g*] isoquinoline (20). The tetrahydroisoquinoline **8** (120 mg, 0.34 mmol) and 1-bromo-4-nitrobenzene (81 mg, 0.4 mmol) were dissolved in toluene (5 mL) in a flame-dried round-bottom flask under argon. Cs_2CO_3 (219 mg, 0.67 mmol), (±)-BINAP (cat) and $PdCl_2((o\text{-}tolyl)_3P)_2$ (cat) were added under argon. The reaction was heated at 130 °C for 24 h and TLC of the crude mixture (hexane/EtOAc 1:1) indicated formation of a yellow product (R_f = 0.55) and complete consumption of starting material (R_f = 0.10). The crude mixture was evaporated in vacuo and purified by silica gel flash column chromatography (hexane/EtOAc 8:2) to afford the *N*-arylated isoquinoline **20** (52 mg, 33% yield) as a bright yellow solid. R_f = 0.55 (hexane/EtOAc 1:1). M.p. 78-80 ^oC (hexane/EtOAc). IR (film) ν cm^{-1}: 2934 (C-H), 1591, 1502, 1460, 1414 (Ar-H), 1290, 1112 (Ar-O), 1066 (C-O). NMR ^1H ($CDCl_3$, 300 MHz) δ (ppm): 2.83-2.98 (m, 2H, Ar-CH_2-CH_2-N), 3.52-3.61 (m, 2H, Ar-CH_2-CH_2-N), 3.74 (s, 6H, OCH_3 (x 2)), 3.80 (s, 3H, OCH_3), 4.26 (s, 4H, CH_2-O (x 2)), 5.74 (s, 1H, H-6), 6.41 (s, 2H, H-2', H-6'), 6.72 (s, 1H, H-5), 6.77 (d, *J* = 8 Hz, 2H, H-2'', H-6''), 6.89 (s, 1H, H-10), 8.12 (d, *J* = 8Hz, 2H, H-3'', H-5''). NMR ^{13}C ($CDCl_3$, 75.5 MHz) δ (ppm): 27.6 (CH_2, Ar-CH_2-), 45.2 (CH_2, CH_2-N), 56.6 (CH_3, CH_3-O (x 2)), 61.1 (CH_3, CH_3-O), 62.3 (CH, C-6), 64.7 (CH_2, CH_2-O (x 2)), 104.2 (CH, C-2', C-6'), 111.6 (CH, C-3'', C-5''), 116.5 (CH, C-5), 116.9 (CH, C-10), 126.4 (CH, C-2'', C-6''), 128.2 (C, C-5a), 130.1 (C, C-9a), 137.3 (C, C-1'), 138.1 (C, C-4''), 142.5 (C, C-4a), 143.3 (C, C-10a), 153.7 (C, C-3', C-4', C-5'), 153.9 (C, C-1''). MS (EI) (m/z, %): 479 (M+, 7), 311 (M+-$C_9H_{12}O_3$, 100). ($C_9H_{11}O_3$ = 3,4,5-trimethoxyphenyl). HRMS ESI(+) m/z for $C_{26}H_{27}N_2O_7$ [M+H]+ calcd. 479.1818, found: 479.1824.

5.1.15. *N*-(4-Cyanophenyl)-6-(3,4,5-trimethoxyphenyl)-2,3,6,7,8,9-hexahydro[1,4]dioxino[2,3-*g*]isoquinolone (21). The tetrahydroisoquinoline **8** (120 mg, 0.34 mmol) and 1-bromo-4-cyanobenzene (92 mg, 0.50 mmol) were dissolved in toluene (5 mL) in a flame-dried round-bottom flask under argon. Cs_2CO_3 (2.44 mg, 0.67 mmol), (±)-BINAP (cat) and $PdCl_2((o\text{-}tolyl)_3P)_2$ (cat) were added under argon. The reaction was heated at 150 °C under stirring for 72 h and TLC of the reaction mixture (hexane/EtOAc 1:1) indicated formation of a yellow product (R_f = 0.60) and uncomplete

consumption of SM. The crude mixture was concentrated *in vacuo* and purified by silica gel flash column chromatography (hexane/EtOAc 8:2) to afford the desired isoquinoline **21** (92 mg, 60% yield) as a yellow solid. R_f = 0.60 (hexane/EtOAc 1:1). M.p. 72-78 ^oC (hexane/EtOAc). IR (film) ν cm^{-1}: 2924, 2851 (C-H), 2212 (CN), 1603, 1503, 1461, 1413 (Ar-H), 1235 (Ar-O), 1178, 1066 (C-O). NMR ^1H ($CDCl_3$, 300 MHz) δ (ppm): 2.84-2.91 (m, 2H, Ar-C$\underline{H}_2$-CH_2-N), 3.46-3.54 (m, 2H, Ar-CH_2-C$\underline{H}_2$-N), 3.74 (s, 6H, OCH_3 (x 2)), 3.80 (s, 3H, OCH_3), 4.26 (s, 6H, CH_2-O (x 3)), 5.66 (s, 1H, H-6), 6.41 (s, 2H, H-2', H-6'), 6.70 (s, 1H, H-5), 6.79 (d, *J* = 8 Hz, 2H, H-2'', H-6''), 6.86 (s, 1H, H-10), 7.47 (d, *J* = 8 Hz, 2H, H-3'', H-5''). NMR ^{13}C ($CDCl_3$, 75.5 MHz) δ (ppm): 27.6 (CH_2, Ar-$\underline{C}H_2$-CH_2-N), 44.7 (CH_2, CH_2-N), 56.6 (CH_3, CH_3-O (x 2)), 61.1 (CH, C-6), 62.2, (CH_3, CH_3-O), 64.7 (CH_2, CH_2-O (x 2)), 99.0 (C, CN) 104.2 (CH, C-2', C-6'), 112.8 (CH, C-2'', C-6''), 116.4 (CH, C-5), 116.8 (CH, C-10), 120.7 (C, C-4''), 128.4 (C, C-5a), 130.3 (C, C-9a), 133.8 (CH, C-3'', C-5''), 137.6 (C, C-1'), 142.4 (C, C-4a), 143.2 (C, C-10a), 152.2 (C, C-1''), 153.6 (C, C-3', C-4', C-5'). MS (EI) (m/z, %): 458 (M^+, 23), 291 (M^+-$C_9H_{12}O_3$, 100). ($C_9H_{11}O_3$ = 3,4,5-trimethoxyphenyl). HRMS ESI(+) m/z for $C_{27}H_{26}N_2O_5$ $[M+H]^+$ calcd. 459.1920, found: 459.1918.

5.1.16. Ethyl 6-(6-(pyridinyl)-2,3,8,9-tetrahydro-[1,4]dioxino[2,3-*g*]isoquinolin-7(6*H*)-yl)carboxylate (22). The title compound was prepared, using a similar procedure to that described for the synthesis of **11** starting from the isoquinoline **9** (60 mg, 0.22 mmol), Et_3N (0.1 mL, 0.67 mmol) and ethyl chloroformate (0.05 mL, 0.24 mmol) dissolved in CH_2Cl_2 (12 mL) in 43% yield (33 mg) as a white solid. M.p. 114-115 ºC. IR (film) ν cm^{-1}: 2931, 1695, 1504, 1296 (Ar-O), 1067 (C-O). NMR ^1H ($CDCl_3$, 200 MHz) δ (ppm): 1.26 (t, *J* = 7 Hz, 3H, CH_3-), 2.44-2.47 (m, 1H, CH_2), 2.62-2.65 (m, 1H, CH_2), 2.80-2.83 (m, 1H, -CH_2), 3.22-3.31 (m, 1H, CH_2), 4.18 (s, 1H, H-6), 4.19-4.25 (m, 4H, O-CH_2-CH_2-O), 6.47 (s, 1H, H-5), 6.70 (s, 1H, H-10), 7.14 (d, *J* = 6 Hz, 2H, pyridine), 8.50 (d, *J* = 6 Hz, 2H, pyridine). NMR ^{13}C ($CDCl_3$, 50.4 MHz) δ (ppm): 14.7 (CH_2), 27.6 (CH_2), 39.0 (CH_2), 56.4 (CH-Ar), 61.8 (CH_2, O-CH_2-CH_3), 64.3 (CH_2, -CH_2-O), 64.4 (CH_2, -CH_2-O), 116.4 (CH, C-5), 116.9 (CH, C-10), 122.8 (CH x 2, pyridine), 128.0 (C, C-9a), 130.1 (C, C-5a), 141.5 (C-10a), 142.0 (C-4a), 149.7 (CH x 2, pyridine), 151.2 (C-1' pyridine), 178.1 (C=O). HRMS ESI(+) m/z for $C_{19}H_{21}N_2O_4$ $[M+H]^+$ calcd. 341.1501, found: 341.1498.

5.1.17. Methyl 6-(6-(pyridinyl)-2,3,8,9-tetrahydro-[1,4]dioxino[2,3-*g*]isoquinolin-7(6*H*)-

yl)hexanoate (23). The title compound was prepared, using a similar procedure to that described for the synthesis of **17** starting from the isoquinoline **9** (150 mg, 0.56 mmol), Et_3N (0.3 mL, 2.01 mmol) and methyl bromohexanoate (175 mg, 0.84 mmol) dissolved in DMF (10 mL) in 42% yield (93 mg) as a white solid. M.p. 111-112 ºC. IR (film) ν cm^{-1}: 2933, 1734, 1504, 1299 (Ar-O), 1072 (C-O). NMR ^1H ($CDCl_3$, 200 MHz) δ (ppm): 1.27 (t, *J* = 7 Hz, 2H, CH_2-), 1.49-1.54 (m, 2H, CH_2-), 2.21-2.29 (m, 4H, CH_2-), 2.36-2.46 (m, 2H, N-CH_2), 2.60-2.62 (m, 1H, CH_2), 2.90-2.98 (m, 2H, -CH_2), 3.02-3.18 (m, 1H, CH_2), 3.65 (s, 3H,CH_3O), 4.15-4.18 (m, 4H, O-CH_2-CH_2-O), 4.40 (s, 1H, H-6), 6.16 (s, 1H, H-5), 6.27 (s, 1H, H-10), 7.21 (d, *J* = 6.2 Hz, 2H, Ar), 8.52 (d, *J* = 6.2Hz, 2H, Ar). NMR ^{13}C ($CDCl_3$, 50.4 MHz) δ (ppm): 24.8 (CH_2), 26.3 (CH_2), 26.6 (CH_2), 28.0 (CH_2), 29.7 (CH_2), 46.9 (CH_2-COO-), 54.1 (CH_2), 64.2 (CH_2, O-CH_2-), 64.3 (CH_2, -CH_2-O), 67.3 (CH-Ar), 116.4 (CH, C-5), 116.6 (CH, C-10), 124.9 (CH x 2, pyridine), 127.8 (C, C-9a), 129.3 (C, C-5a), 141.5 (C-10a), 142.0 (C-4a), 148,3 (CH x 2, pyridine), 154.9 (C-1' pyridine), 177.2 (COOH). HRMS ESI(+) m/z for $C_{24}H_{31}N_2O_4$ $[M+H]^+$ calcd. 411.2284, found: 411.2288.

5.1.18. 6-(6-(Pyridin-4-yl)-2,3,8,9-tetrahydro-[1,4]dioxino[2,3-*g*]isoquinolin-7(6*H*)-yl)hexanoic acid (24). The title compound was prepared, using a similar procedure to that described for the synthesis of **18** starting from the isoquinoline **23** (30 mg, 0.10 mmol) and NaOH in 74% yield (35 mg) as a white solid. M.p. 57-58 ºC. IR (film) ν cm^{-1}: 2927, 1716, 1603, 1505, 1299 (Ar-O), 1066 (C-O). NMR ^1H ($CDCl_3$, 200 MHz) δ (ppm): 1.25 (t, *J* = 7 Hz, 2H, CH_2-), 1.49 (qt, *J* = 7 Hz, 2H, CH_2-), 2.24-2.29 (m, 4H, CH_2-), 2.38-2.47 (m, 2H, N-CH_2), 2.80-2.82 (m, 1H, CH_2), 2.91-3.09 (m, 2H, -CH_2), 3.12-3.21 (m, 1H, CH_2), 4.13-4.20 (m, 4H, O-CH_2-CH_2-O), 4.43 (s, 1H, H-6), 6.12 (s, 1H, H-5), 6.62 (s, 1H, H-10), 7.29 (d, *J* = 6.2 Hz, 2H, Ar), 7.98 (bs, 2H, Ar); 8.42 (bs, 1H, COOH). NMR ^{13}C ($CDCl_3$, 50.4 MHz) δ (ppm): 24.8 (CH_2), 26.6 (CH_2), 26.7 (CH_2), 27.9 (CH_2), 34.0 (CH_2), 46.9 (CH_2-COO-), 54.2 (CH_2), 64.3 (CH_2, O-CH2-), 64.4 (CH_2, -CH_2-O), 67.2 (CH-Ar), 116.3 (CH, C-5), 116.7 (CH, C-10), 124.4 (CH x 2, pyridine), 127.9 (C, C-9a), 129.5 (C, C-5a), 141.5 (C-10a), 142.0 (C-4a), 149,5 (CH x 2, pyridine), 153.7 (C-1' pyridine), 173.9 (COOH). HRMS ESI(+) m/z for $C_{22}H_{27}N_2O_4$ [M+H]+ calcd. 383.1971, found: 383.1973.

5.1.19. 2-(6,7-Dimethoxy-1-(3,4,5-trimethoxyphenyl)-1,2,3,4-tetrahydroisoquinoline)ethanol (25). From the tetrahydroisoquinoline **27** (150 mg, 0.42 mmol) and 2-bromoethanol (0.06 mL, 0.83

mmol), and following the general procedure described above the title compound was obtained (82 mg, 49% yield) as a white solid. R_f = 0.65 (EtOAc/MeOH 8:2). M.p. 77-80 ^oC (EtOAc). IR (film) ν cm^{-1}: 3516 (OH), 2937, 2834 (C-H), 1591, 1516, 1423 (Ar-H), 1257, 1221 (Ar-O), 1121 (C-O). NMR ^1H ($CDCl_3$, 300 MHz) δ (ppm): 2.40-2.52 (m, 1H, C$\underline{H}_2$-Ar), 2.52-2.65 (m, 1H, C$\underline{H}_2$-Ar), 2.70-2.85 (m, 2H, C$\underline{H}_2$-N), 2.85-3.00 (m, 1H, C$\underline{H}_2$-N), 3.10-3.25 (m, 1H, C$\underline{H}_2$-N), 3.40-3.55 (m, 1H, CH_2-OH), 3.61 (s, 3H, CH_3-O), 3.62-3.70 (m, 1H, CH_2-OH), 3.76 (s, 6H, CH_3-O (x 2)), 3.81 (s, 3H, CH_3-O), 3.82 (s, 3H, CH_3-O), 4.45 (s, 1H, H-1), 6.22 (s, 1H, H-5), 6.41 (s, 2H, H-2', H-6'), 6.58 (s, 1H, H-8). NMR ^{13}C ($CDCl_3$, 75.5 MHz) δ (ppm): 28.1 (CH_2, $\underline{C}H_2$-Ar), 46.9 (CH_2, $\underline{C}H_2$-N), 55.4 (CH_2, $\underline{C}H_2$-N), 56.1 (CH_3, OCH_3), 56.2 (CH_3, OCH_3), 56.5 (CH_3, OCH_3 (x 2)), 58.5 (CH_2, $\underline{C}H_2$-OH), 61.2 (CH_3, OCH_3), 68.6 (CH, C-1), 106.7 (CH, C-2', C-6'), 111.1 (CH, C-5), 111.8 (CH, C-8), 126.8 (C, C-4a), 129.4 (C, C-8a), 139.6 (C, C-1'), 147.4 (C, C-7), 147.9 (C, C-6), 153.4 (C, C-3', C-4', C-5'). MS EI m/z (%): 403 (M^+, 11), 372 (M^+-C_2H_8, 100), 236 (M^+-$C_9H_{12}O_3$, 77). ($C_9H_{11}O_3$ = 3,4,5-trimethoxyphenyl). HRMS ESI(+) m/z for $C_{22}H_{30}NO_6$ $[M+H]^+$ calcd. 404.2073, found: 404.2076.

5.1.20. 3-(6,7-Dimethoxy-1-(3,4,5-trimethoxyphenyl)isoquinolin-2-yl)-1,2-propanediol (26).

First step: preparation of the intermediate 6,7-Dimethoxy-*N*-(oxirane-2-yl-methyl)-1-(3,4,5-trimethoxyphenyl)-1,2,3,4-tetrahydroisoquinoline. From the tetrahydroisoquinoline **27** (100 mg, 0.28 mmol) and epichlorohydrin (0.2 mL, 2.55 mmol), and following the classical procedure for the *N*-alkylation, agitation of the mixture at room temperature during 24 h the title compound was obtained (52 mg, 45% yield) as an orange solid. R_f = 0.30 (hexane/EtOAc 2:8). IR (film) ν cm^{-1}: 2920, 2849 (C-H), 1586, 1503, 1450, 1410 (Ar-H), 1221 (Ar-O), 1120, 1002 (C-O). NMR ^1H ($CDCl_3$, 300 MHz) δ (ppm): 2.50-3.10 (m, 9H, C$\underline{H}_2$-CH_2-N, C$\underline{H}_2$-N (x 2), C$\underline{H}$-O (x 2), CH_2-O), 3.65 (s, 3H, CH_3-O), 3.81 (s, 6H, CH_3-O (x 2)), 3.85 (s, 3H, CH_3-O), 3.87 (s, 3H, CH_3-O), 4.60 (s, 1H, H-1), 6.25 (s, 2H, H-2', H-6'), 6.48 (s, 1H, H-5), 6.63 (s, 1H, H-8).

The oxirane (50 mg) was treated with NaOH 2N in 1,4-dioxane (10 and 4 mL respectively) and the solution was stirred 48 h at room temperature. The crude mixture was extracted with dichoromethane (3 x 10 mL), dried, filtered and concentrated in vacuo. The residue was purified by silica gel flash column chromatography (hexane/EtOAc 8:2) to afford the diol **26** as a brown solid (48% yield). R_f = 0.60 (hexane/EtOAc 8:2). M.p. 70-73 ºC (hexane/EtOAc). IR (film) ν cm^{-1}: 3700-3050 (OH), 2919,

2849 (C-H), 1505, 1461, 1452, 1415 (Ar-H), 1215 (Ar-O), 1120 (C-O). NMR ^{1}H ($CDCl_3$, 300 MHz) δ (ppm): 2.60-3.25 (m, 9H, C<u>H</u>$_2$-CH_2-N, C<u>H</u>$_2$-N (x 2), C<u>H</u>-O (x 2), CH_2-O), 3.73 (s, 3H, CH_3-O), 3.81 (s, 6H, CH_3-O (x 2)), 3.84 (s, 3H, CH_3-O), 3.87 (s, 3H, CH_3-O), 4.18 (s, 1H, H-1), 6.58 (s, 1H, H-5); 6.80 (s, 2H, H-2', H-6'), 6.85 (s, 1H, H-8). NMR ^{13}C ($CDCl_3$, 75.5 MHz) δ (ppm): 30.0 (CH_2, Ar-C<u>H</u>$_2$), 47.9 (CH_2, CH_2-N), 54.3 (CH_2); 56.1 (CH_3, CH_3-O), 56.4 (CH_3, OCH_3), 56.5 (CH_3, OCH_3 (x 2)), 61.1 (CH_3, OCH_3), 65.0 (CH_2), 75.8 (CH, C-1), 76.7 (CH, CH-OH), 104.2 (CH, C-2', C-6'), 111.6 (CH, C-5), 126.9 (C, C-8a), 128.7 (C, C-4a), 140.7 (C, C-1'), 147.8 (C, C-7), 148.7 (C, C-6), 153.5 (C, C-4'), 153.3 (C, C-3', C-5'). HRMS ESI(+) m/z for $C_{23}H_{31}NO_7$ $[M+H]^+$: calcd. 433.2101, found: 433.2156.

5.1.21. 6,7-Dimethoxy-1-(3,4,5-trimethoxyphenyl)-1,2,3,4-tetrahydroisoquinoline (27). The acyl-isoquinoline **28** (870 mg, 1.91 mmol) was dissolved in MeOH (15 mL). NaOH 2N (45 mL) was added and the reaction was heated to reflux for 16 h. Then, TLC of the crude mixture (hexane/EtOAc 1:1) showed total consumption of Starting material (R_f = 0.75) and formation of a new compound (R_f = 0.15). The methanol was evaporated *in vacuo*. The aqueous phase was extracted with CH_2Cl_2 (3 x 20 mL) and the combined organic phases were dried (Na_2SO_4), filtered and concentrated *in vacuo.* The crude residue was purified by flash column chromatography (hexane/EtOAc 1:1) to afford the desired isoquinoline **27** (480 mg, 70% yield) as a white solid. R_f = 0.15 (hexane/EtOAc 1:1). M.p. 95-97 ^{o}C (EtOAc). IR (film) ν cm^{-1}: 3310 (NH), 3002-2828 (C-H), 1736 (C=O), 1590, 1515, 1504, 1461, 1420 (Ar-H), 1251, 1226, 1214 (Ar-O), 1123, 1111 (C-O). NMR ^{1}H ($CDCl_3$, 300 MHz) δ (ppm): 2.65-2.78 (m, 1H, C<u>H</u>$_2$-CH_2-N), 2.90-3.10 (m, 2H, H-C-4, H-C-3) 3.20-3.30 (m, 1H, C<u>H</u>$_2$-N), 3.68 (s, 3H, CH_3-O), 3.81 (s, 6H, CH_3-O (x 2)), 3.85 (s, 3H, CH_3-O), 3.88 (s, 3H, CH_3-O), 4.97 (s, 1H, H-1), 6.31 (s, 1H, H-5), 6.49 (s, 2H, H-2', H-6'), 6.63 (s, 1H, H-8). NMR ^{13}C ($CDCl_3$, 75.5 MHz) δ (ppm): 29.0 (CH_2, Ar-C<u>H</u>$_2$), 39.7 (CH_2, CH_2-N), 56.2 (CH_3, CH_3-O), 56.3 (CH_3, OCH_3), 56.5 (CH_3, OCH_3 (x 2)), 56.8 (CH3, OCH_3), 61.1 (CH, C-1), 106.6 (CH, C-2', C-6'), 111.3 (CH, C-5), 111.4 (CH, C-8), 125.2 (C, C-4a), 126.1 (C, C-8a), 136.8 (C, C-1'), 148.2 (C, C-7), 148.9 (C, C-6), 153.5 (C, C-3', C-4', C-5'). HRMS ESI(+) m/z for $C_{20}H_{26}NO_5$ $[M+H]^+$: calcd. 360.1811, found: 360.1814.

5.1.22. (6,7-Dimethoxy-1-(3,4,5-trimethoxyphenyl)-1,2,3,4-tetrahydroisoquinolin-2-yl)2,2,2-

trifluoro acetate (28). The homoveratrylamine **29** (2 g, 11 mmol) and 3,4,5-trimethoxybenzaldehyde (**4**) (2.38 g, 12.1 mmol) were dissolved in toluene (30 mL) in a flame-dried round-bottom flask under argon. PTSA (catalytic amount) and 4 Å molecular sieves (50 mg) were added. The reaction mixture was heated to reflux under stirring for 16 h and TLC of the reaction mixture (EtOAc) indicated the presence of the aldehyde (R_f = 0.80) and the imine (R_f = 0.85). The crude mixture was filtered to afford 5 g of brown oil. CF_3COOH (7 mL) and $(CF_3CO)_2O$ (7 mL) were added and the mixture was stirred for 24 h. TLC of the crude mixture (EtOAc/hexane 1:1) indicated the presence of the desired compound (R_f = 0.75) and complete consumption of the imine. The crude reaction was dissolved in EtOAc (20 mL), washed with NaOH 2N (3 x 30 mL) and the combined aqueous phases were re-extracted with EtOAc (3 x 20 mL). The combined organic phases were dried (Na_2SO_4), filtered and concentrated *in vacuo*. The residue was purified by silica gel flash column chromatography (hexane/EtOAc 1:1) to afford the desired compound **28** (1.67 g, 33% yield) as a pale brown oil. R_f = 0.75 (hexane/EtOAc 1:1). NMR ^{1}H ($CDCl_3$, 300 MHz) δ (ppm): 2.70-2.85 (m, 2H, Ar-C<u>H</u>$_2$-CH_2-N), 2.90-3.10 (m, 1H, Ar-C<u>H</u>$_2$-CH_2-N), 3.35-3.50 (m, 1H, CH_2-N), 3.68 (s, 3H, CH_3-O (x 2)), 3.71 (s, 3H, CH_3-O), 3.77 (s, 3H, CH_3-O), 3.83 (s, 3H, CH_3-O), 3.85-3.95 (m, 1H, CH_2-N), 6.39 (s, 2H, H-2', H-6'), 6.46 (s, 1H, H-5), 6.61 (s, 1H, H-1) 6.62 (s, 1H, H-8). NMR ^{13}C ($CDCl_3$, 75.5 MHz) δ (ppm): 28.9 (CH_2, CH_2-Ar), 39.6 (CH_2, CH_2-N), 56.1 (CH_3, OCH_3), 56.3 (CH_3, OCH_3), 56.4 (CH_3, OCH_3 (x 2)), 56.8 (CH_3, OCH_3), 61.0 (CH, C-1), 106.5 (CH, C-2', C-6'), 111.2 (CH, C-8), 111.3 (CH, C-5), 116.5 (C, *J* = 288 Hz, CF_3), 125.1 (C, C-4a), 125.9 (C, C-8a), 136.8 (C, C-1'), 148.1 (C, C-7), 148.8 (C, C-6), 153.5 (C, C-3', C-4', C-5'), 156.0 (C, *J* = 36 Hz, C=O). MS EI m/z (%): 455 (M^+, 34), 357 (M^+-C_2F_3O, 100).

5.2. Molecular modeling methods

The 3D structure of the KRas protein was obtained from the Protein Data Bank server (PDB) with ID code 4DSN.1 Bond orders and protonation states of the protein were automatically adjusted by using the Protein Preparation Wizard workflow included in the Maestro v.10.0 software package [14]. The GCP (phosphomethylphosphonic acid guanylate ester) cofactor was manually modified to be transformed in the GTP (guanosine triphosphate) cofactor. All calculations were done with the AMBER v.14 software package [15] using the PMEMD program in its CPU and GPU versions. The

ff14SB [16] and the GAFF [17] force fields were used for the protein and the ligands, respectively. Force field parameters for GTP was obtained from Meagher et al. [18].

5.2.1. Generation of KRas-Lig8 complexes

Complexes formed by the KRas receptor and eight ligands (KRas-Lig8) were prepared as follows: first the protein was oriented using the Principal Axes of Inertia in order Ia <= Ib <= Ic . Second, a rectangular box around the protein was created whose size in each dimension was obtained adding to the protein size (x_boxprot, y_boxprot, z_boxprot) the maximum distance between ligand atoms (dis_lig) and a buffer of two times a minimum box size (min_box) that was set to 5 Å in all calculations (Figure S1a in Supporting Information). Next, the resulting box was discretized using an interval dimension of 2 Å (Figure S1b in Supporting Information), and an exclusion area was determined to avoid putting the ligands inside the protein or near the edges of the cube (Figure S1c in Supporting Information). Finally, for each quadrant the position of the ligand center of masses was generated randomly. If none of the ligand atoms falls in the forbidden space the position is accepted, otherwise new random points are generated until a good position is obtained (Figure S1d in Supporting Information). Once the initial ligand position is determined a local rotation is performed randomly and possible clashes with the forbidden positions tested again.

5.2.2. Molecular dynamics (MD) simulations

Complexes KRas-Lig_8 and KRas-Lig were prepared with the leap module of Ambertools v.16. [19] An identical protocol was followed for all complexes. Structures were neutralized with counterions following a grid-shaped procedure for mapping electrostatic potential surface. Finally, a cubic box of TIP3P waters [20] was created with a minimum distance between any atom of the system and the edge of the box of 15 Å and removing water molecules closer than 2.0 Å to any of the atoms.

The prepared structures were heated at 300 K at a constant rate of 30 K/10 ps with harmonic restrains of 5 kcal/mol/$Å^2$ in the protein main atoms. Once the systems were heated, 500 ps at constant pressure were performed to increase the system density using harmonic restrains of 1 kcal/mol/$Å^2$ in the protein main atoms. Finally, different production molecular dynamic simulations were done under the canonical ensemble using Langevin [21] thermostat with a collision frequency

of 2 ps^{-1} for temperature control. Long-range electrostatic energy was computed using the Particle Mesh Ewald summation method [22] with a cutoff of 9 Å for non-bonded interactions. SHAKE algorithm [23] was used to constrain the bonds involving the hydrogen atoms and to allow an integration time of 2 fs.

Ten KRas-Lig_8 complexes were generated as explained before and for each of them 100 ns of production MD was carried out. In order to analyze more in deep all the binding sites located in the multiple-ligands MD, we generated eighteen complexes extracted at the end these calculations by removing all waters, ions and ligands that were not bonded to the KRas protein during the last ten ns of the MD and keeping only one ligand in each complex. To prepare the eighteen complexes the same procedure as for the KRas-Lig_8 was used. The length of the production runs for these last complexes ranges between 100 and 700 ns depending on the evolution of each system leading to a total production time of 4.7μs.

5.2.3. MMGBSA Calculations

The calculation and decomposition of the binding free energy, $\Delta G_{binding}$, for all the studied protein-ligand complexes were evaluated using the MMGBSA (molecular mechanics generalized Born surface area) method as implemented in Ambertools v.16. [18] In this approach, the total binding free energy is calculated as $\Delta G_{binding} = \Delta H^0_{gas} - T\Delta S^0 + \Delta G_{solv}$, where ΔH^0_{gas}, the gas phase interaction energy, is calculated as the sum of the internal energy (ΔH^0_{int}) and two non-bonded terms corresponding to the van der Waals (ΔH^0_{vdW}) and electrostatic (ΔH^0_{elec}) molecular mechanics energies: $\Delta H^0_{gas} = \Delta H^0_{int} + \Delta H^0_{vdW} + \Delta H^0_{elec}$. The solvation free energy (ΔG_{solv}) is obtained by summing the polar (ΔG_{polar}) and nonpolar ($\Delta G_{nonpolar}$) terms: $\Delta G_{solv} = \Delta G_{polar} + \Delta G_{nonpolar}$. The ΔG_{polar} is calculated using the Generalized Born method. In this work, we used the Onufriev- Bashford-Case (OBC) generalized Born [24] (igb = 5) as implemented in Ambertools v.16. The nonpolar contribution ($\Delta G_{nonpolar}$) is calculated from the solvent accessible surface area (SASA) according to the equation: $\Delta G_{nonpolar} = \gamma$ SASA + β where the values for γ and β were set to 0.0072 kcal / mol $Å^2$ and 0 kcal / mol [25]. Values for interior and exterior dielectric constants were set to 1 and 80, respectively. In order to assess the convergence and stability of the $\Delta G_{binding}$ values along the time, MMGBSA computations were performed for the complete MD simulations taking 50 structures each

nanosecond using the cpptraj program as implemented in Ambertools v.16. The contribution of the receptor residues to the total binding free energy was obtained for the last 20 ns using a total of 1000 structures.

5.3. Biological Experimental

5.3.1. Inhibition Growth Rate Determination

L1210 leukemia cells were grown in nutrient medium RPMI 1640 supplemented with 2 mM L-glutamine, 200 IU/mL penicillin, 50 μg/mL streptomycin, and 20% heat inactivated horse serum. They were incubated in a 5% CO_2 atmosphere at 37 ºC. For the experiments the drugs were dissolved in dimethyl sulfoxide (0.5% final) and added to the cells in exponential phase of growth at an initial concentration of 0.8 x 10^5 cells/mL. The cells were counted in triplicate after 48 h with Coultronics Coulter Counter and results were expressed as the drug concentration which inhibited cell growth by 50% as compared to the controls (IC_{50}). The IC_{50} values were calculated from regression lines obtained from the probit of the percent cell growth inhibition plotted as a function of the logarithm of the dose [26].

5.3.2. Inhibition of Cellular Proliferation and Cell Cycle Effects

L1210 leukemia cells were grown in nutrient medium RPMI 1640 supplemented with 2 mM L-glutamine, 200 IU/mL penicilium, 50 μg/mL streptomicyn, and 20% heat inactivated horse serum. They were incubated in a 5% CO_2 atmosphere at 37 ºC for 21 h with several drug concentrations. Cells were then fixed by ethanol (70% v/v), then washed, and incubated with PBS containing 100 μM RNAse and 25 μM/mL propidium iodide for 30 min at room temperature. For each concentration, 10-4 cells were analysed on an Epics XL flow cytomer (Modele Beckman Coulter, French). Results were expressed as a percentage of cells accumulated in each phase of the cell cycle and are indicated.

5.3.3. OIDD Lilly Tests

The Lilly tests (KRas inhibition and antiangiogenesis activities) were carried out according the procedures indicated in the OIDD-Lilly program (Open Innovation Drug Discovery - Eli Lilly) (https://openinnovation.lilly.com).

Supporting Information Available: (see footnote on the first page of this article): Additional Molecular studies data, Copies of ^{1}H and ^{13}C NMR spectra of all new compounds. This material is available free of charge via the internet at http://dx.doi.org/ejmech

Acknowledgements

OIDD screening data supplied courtesy of Eli Lilly and Company—used with Lilly's permission. The Spanish Minister (CTQ2011-29285-C02-02) and the SGR(2014)-1017 Generalitat de Catalunya and the Laboratories Servier (France) are gratefully acknowledged for their financial support.

Author Information

Corresponding Author:

*Address correspondence to: Maria Dolors Pujol; Av. Diagonal 643, 08028-Barcelona, Spain. Phone, +34-93-4024534; fax, +34-93-4035941. E-mail: mdpujol@ub.edu

Abbreviations

IC_{50}, inhibitory concentration at 50% inhibition; BINAP, 2,2'-*bis*(diphenylphosphino)-1,1'-binaphthyl; DCM, dichloromethane; DMF, dimethylformamide; ESI, electrospray; HMRS, high resolution mass spectrometry; KRAS, Kirsten rat sarcoma viral oncogene homolog; NMR, nuclear magnetic resonance, PDA, protein data bank; TLC, thin layer chromatography, TFA, trifluoro acetic acid, TFAA, trifluoro acetic anhydride.

References

[1] a) M. E. Welsch, S. A. Snyder, B. R. Stockwell, Privileged scaffolds for library design and drug discovery, Curr. Opin. Chem. Biol. 14 (2010) 347-361. b) Singh, H.; Singh, P.; Kumari, K.;

Chandra, A.; Dass, S. K.; Chandra, R. A review on noscapine, and its impact on hemo metabolism, Curr. Drug Metab. 14 (2013) 351–360. PMID 22935070. c) F. Grande, G. Giancotti, G. Ioele, M. A. Occhiuzzi, A. Garofalo. An update on small molecules targeting CXCR4 as starting points for the development of anti-cancer therapeutics. Eur. J. Med. Chem. 139(2017) 519-530. d) J. Tang, S. K. V. Vernekar, Y.-L. Chen, L. Miller, A. D. Huber, N. Myshakina, S. G. Sarafianos, M. A. Parniak, Z. Wang. Synthesis, biological evaluation and molecular modeling of 2-Hydroxyisoquinoline-1,3-dione analogues as inhibitors of HIV reverse transcriptase associated ribonuclease H and polymerase. Eur. J. Med. Chem. 133(2017) 85-96. e) D. N. Karelia, U. Hossain Sk, P. Singh, A. S. P. Gowda, M. K. Pandey, S. R. Ramisetti, S. Amin, A. K.Sharma. Design, synthesis, and identification of a novel napthalamide-isoselenocyanate compound NISC-6 as a dual Topoisomerase-IIα and Akt pathway inhibitor, and evaluation of its anti-melanoma activity. Eur. J. Med. Chem. 135(2017) 282-295. f) I. P. Singh, P. Shah. Tetrahydroisoquinolines in therapeutics: a patent review (2010-2015). Expert Opin. Ther. Pat. 27(2017), 17-36.

[2] a) N. Cabedo, I. Berenguer, B. Figadère, D. Cortes. An overview on benzylisoquinoline derivatives with dopaminergic and serotonergic activities. Curr. Med. Chem. 16(2009) 2441-2467. b) P. Zhu, W. Ye, J. Li, Y. Zhang, W. Huang, M. Cheng, Y. Wang, Y. Zhang, H. Liu, J. Zuo. Design, synthesis, and biological evaluation of novel tetrahydroisoquinoline derivatives as potential antitumor candidate. Chem. Biol. Drug Des. 89(2017) 443-455. c) J. W. Seo, E. Srisook, H. J. Son, O. Hwang, Y.-N. Cha, D. Y. Chi. Syntheses of tetrahydroisoquinoline derivatives that inhibit NO production in activated BV-2 microglial cells. Eur. J. Med. Chem. 43(2008) 1160-1170.

[3] Y. Ko, D. C. Malone, E. P. Armstrong, Pharmacoeconomic evaluation of antimuscarinic agents for the treatment of overactive bladder. Pharmacotherapy 26 (2006) 1694–702. doi: 10.1592/phco.26.12.1694.

[4] Z. Xie, L. Liu, W. Chen, H. Zheng, Q. Xu, H. Yuan, H. Lou, Practical Metal-Free C(sp3)[BOND]H Functionalization: Construction of Structurally Diverse α-Substituted *N*-Benzyl and *N*-Allyl Carbamates, Angew. Chem. Int. Ed. 53 (2014) 3904-3908.

[5] R. Patil, S. Patil, X. D. Wang, F. Ma, W. E. Orr, W. Li, C. R. Yates, E. E. Geisert, D. D. Miller, Synthesis and evaluation of new 1,2,3,4-tetrahydroisoquinoline analogs as antiglioma agents, Med. Chem. Res. 20 (2011) 131-137.

[6] a) M. L. Mohler, G. S. Kang, S. S. Hong, R. Patil, O. V. Kirichenko, W. Li, I. M. Rakov, E. E. Geisert, D. D. Miller, Discovery of Antiglioma Activity of Biaryl 1,2,3,4-Tetrahydroisoquinoline Derivatives and Conformationally Flexible Analogues, J. Med. Chem. 49 (2006) 5845-5848, b) L. Li, J. Feng, T. Wu, P. Ren, Y. Liu, Y. Liu, Y. O. Long, Preparation of nitrogen-containing heterobicycles as inhibitors of KRAS G12C, PCT Int. Appl. 2015, WO 2015054572 A1 20150416, c) L.-N. Wen, M.-X.Xie, Spectrochim. Acta A Mol. Biomol. Spectrosc. 171 (2017) 287-296.

[7] J. J. Li, Name Reactions: A Collection of detailed Mechanism and synthetic Applications. Springer International Switzerland 2014, 56-58. DOI: 10.1007/978-3-03979-4_27.

[8] a) A. S. Capilla, M. Romero, M. D. Pujol, D. H. Caignard, P. Renard, Synthesis of Isoquinolines and Tetrahydroisoquinolines as Potential Antitumor Agents, Tetrahedron 57 (2001) 8297-8303, b) M. Romero, D. H. Caignard, P. Renard, M. D. Pujol, Synthesis of tetracyclic dioxygenated isoquinolines and their cytotoxic activity, Tetrahedron 64 (2008) 11020-11027.

[9] J. Rodriguez, M. D. Pujol, Straightforward synthesis of nitroolefins by microwave- or ultrasound-assisted Henry reaction, Tetrahedron Lett. 52 (2011) 2629-2632.

[10] a) Y. Harrak, M. Romero, P. Constans, M. D. Pujol, Preparation of Diarylamines and Arylhydrazines Using Palladium Catalysts, Lett. Org. Chem. 3 (2006) 29-35, b) M. Romero, Y. Harrak, J. Basset, L. Ginet, P. Constans, M. D. Pujol, Preparation of N-arylpiperazines and other N-aryl compounds from aryl bromides as scaffolds of bioactive compounds, Tetrahedron 60 (2006) 9010-9016.

[11] https://openinnovation.lilly.com/dd/about-open-innovation/resources-links.html.

[12] J. J. Perez, M. S. Tomas, J. Rubio-Martinez, Assessment of the Sampling Performance of Multiple-Copy Dynamics versus a Unique Trajectory, J. Chem. Inf. Model. 56 (2016) 1950-1962.

[13] T. Maurera, L. S. Garrenton, A. Oh, K. Pitts, D. J. Anderson, N. J. Skelton, B. P. Fauber, B. Pan, S. Malek, D. Stokoe, M. J. C. Ludlam, K. K. Bowman, J. Wu, A. M. Giannetti, M. A. Starovasnik, I. Mellman, P. K. Jackson, J. Rudolph, W. Wang, G. Fang, Small-molecule ligands bind to a distinct pocket in Ras and inhibit SOS-mediated nucleotide exchange activity, PNAS 109 (2012) 5299-5304.

[14] Schrödinger Release 2014-4: Maestro, version 10.0, Schrödinger, LLC, New York, NY, 2014.

[15] D. Case, V. Babin, J. Berryman, R. Betz, Q. Cai, D. Cerutti, T. E. Cheatham, T. Darden, R. Duke, H. Gohlke, A. Goetz, S. Gusarov, N. Homeyer, P. Janowski, J. Kaus, I. Kolossvary, A. Kovalenko, T. Lee, S. LeGrand, T. Luchko, R. Luo, B. Madej, K. Merz, F. Paesani, D. Roe, A. Roitberg, A.; C. Sagui, R. Salomon-Ferrer, G. Seabra, C. Simmerling, W. Smith, J. Swails, R. Walker, J. Wang, R. Wolf, X. Wu, P. Kollman, AMBER 14, 2014; University of California, San Francisco.

[16] J. A. Maier, C. Martinez, K. Kasavajhala, L. Wickstrom, J. E. Hauser, C. Simmerling, C. f14SB: Improving the Accuracy of Protein Side Chain and Backbone Parameters from ff99SB, J. Chem. Theory Comput. 11 (2015) 3696-3713.

[17] J. Wang, R. M. Wolf, J. W. Caldwell, P. A. Kollman, D. A. Case, Development and testing of a general amber force field, J. Comput. Chem. 25 (2004) 1157–1174.

[18] Meagher, K.L.; Redman, L.T.; Carlson, H.A. Development of polyphosphate parameters for use with the AMBER force field. J. Comput. Chem. 24 (2003) 1016-1025.

[19] D. Case, R. Betz, W. Botello-Smith, D. S. Cerutti, T. E. Cheatham, T. Darden, R. E. Duke, T. J. Giese, H. Gohlke, A. Goetz, N. Homeyer, S. Izadi, P. Janowski, J. Kaus, A. Kovalenko, T. Lee, S. LeGrand, P. Li, C. Lin, T. Luchko, R. Luo, B. Madej, D. Mermelstein, K. Merz, G. Monard, H. Nguyen, H. T. Nguyen, I. Omelyan, A. Onufriev, D. R. Roe, A. Roitberg, C. Sagui, C. Simmerling, J. Swails, R. C. Walker, J. Wang, R. M. Wolf, X. Wu, L. Xiao, York, D. M.; Kollman, P. *AMBER* 2016. University of California, San Francisco.

[20] W. L. Jorgensen, J. Chandrasekhar, J. D. Madura, R. W. Impey, M. L. Klein, Comparison of simple potential functions for simulating liquid water, J. Chem. Phys. 79 (1983) 926-935.

[21] B. P. Uberuaga, M. Anghel, A. F. Voter, Synchronization of trajectories in canonical molecular-dynamics simulations: observation, explanation, and exploitation, J. Chem. Phys. 120 (2004) 6363-6374.

[22] T. Darden, D. York, L. Pedersen, Particle Mesh Ewald: An N.Log(N) Method for Ewald Sums in Large Systems, J. Chem. Phys. 98 (1993) 10089-10092.

[23] J. P. Ryckaert, G. Ciccotti, H. J. C. Berendsen, Numerical Integration of the Cartesian Equations of Motion of a System with Constraints: Molecular Dynamics of *n*-alkanes, J. Comput. Phys. 23 (1977) 327-341.

[24] A. Onufriev, D. Bashford, D. A. Case, Exploring protein native states and largescale conformational changes with a modified generalized born model, Protein Struct. Funct. Bioinf. 55 (2004) 383-394.

[25] H. Gohlke, D. A. Case, Converging free energy estimates: MMPB(GB)SA studies on the protein-protein complex Ras-Raf, J. Comput. Chem. 25 (2004) 238-250.

[26] K. K. Chiruvella, V. Kari, B. Choudhary, M. Nambiar, R. G. Ghanta, S. C. Raghavan, Methyl angolensate, a natural tetranortriterpenoid induces intrinsic apoptotic pathway in leukemic cells, FEBS Lett. 582 (2008) 4066-4076.

The authors declare no competing financial interest